

Article

Adaptation of Tree Species in the Greater Khingan Range under Climate Change: Ecological Strategy Differences between *Larix gmelinii* and *Quercus mongolica*

Bingyun Du ¹, Zeqiang Wang ¹, Xiangyou Li ¹, Xi Zhang ¹, Xuotong Wang ¹ and Dongyou Zhang ^{1,2,*}

- ¹ Heilongjiang Province Key Laboratory of Geographical Environment Monitoring and Spatial Information Service in Cold Regions, Harbin Normal University, Harbin 150025, China; duby@stu.hrbnu.edu.cn (B.D.); wangzeqiang@stu.hrbnu.edu.cn (Z.W.); hsdlyx1999@gmail.com (X.L.); zhangxi@stu.hrbnu.edu.cn (X.Z.); 18845725592@163.com (X.W.)
- ² Heilongjiang Wuyiling Wetland Ecosystem National Observation and Research Station, Yichun 153000, China
- * Correspondence: zhangdy@hrbnu.edu.cn

Abstract: Global warming significantly affects forest ecosystems in the Northern Hemisphere's mid-to-high latitudes, altering tree growth, productivity, and spatial distribution. Additionally, spatial and temporal heterogeneity exists in the responses of different tree species to climate change. This research focuses on two key species in China's Greater Khingan Range: *Larix gmelinii* (Rupr.) Kuzen. (Pinaceae) and *Quercus mongolica* Fisch. ex Ledeb. (Fagaceae). We utilized a Maxent model optimized by the kuenm R package to predict the species' potential habitats under various future climate scenarios (2050s and 2070s) considering three distinct Shared Socioeconomic Pathways: SSP1-2.6, SSP2-4.5, and SSP5-8.5. We analyzed 313 distribution records and 15 environmental variables and employed geospatial analysis to assess habitat requirements and migration strategies. The Maxent model demonstrated high predictive accuracy, with Area Under the Curve (AUC) values of 0.921 for *Quercus mongolica* and 0.985 for *Larix gmelinii*. The high accuracy was achieved by adjusting the regularization multipliers and feature combinations. Key factors influencing the habitat of *Larix gmelinii* included the mean temperature of the coldest season (BIO11), mean temperature of the warmest season (BIO10), and precipitation of the driest quarter (BIO17). Conversely, *Quercus mongolica*'s habitat suitability was largely affected by annual mean temperature (BIO1), elevation, and annual precipitation (BIO12). These results indicate divergent adaptive responses to climate change. *Quercus mongolica*'s habitable area generally increased in all scenarios, especially under SSP5-8.5, whereas *Larix gmelinii* experienced more complex habitat changes. Both species' distribution centroids are expected to shift northwestward. Our study provides insights into the divergent responses of coniferous and broadleaf species in the Greater Khingan Range to climate change, contributing scientific information vital to conserving and managing the area's forest ecosystems.

Keywords: global warming; Maxent; GIS; potential habitats; parameter optimization



Citation: Du, B.; Wang, Z.; Li, X.; Zhang, X.; Wang, X.; Zhang, D. Adaptation of Tree Species in the Greater Khingan Range under Climate Change: Ecological Strategy Differences between *Larix gmelinii* and *Quercus mongolica*. *Forests* **2024**, *15*, 283. <https://doi.org/10.3390/f15020283>

Academic Editors: Cheng Li, Fei Zhang, Mou Leong Tan and Kwok Pan Chun

Received: 12 December 2023

Revised: 25 January 2024

Accepted: 31 January 2024

Published: 2 February 2024



Copyright: © 2024 by the authors. Licensee MDPI, Basel, Switzerland. This article is an open access article distributed under the terms and conditions of the Creative Commons Attribution (CC BY) license (<https://creativecommons.org/licenses/by/4.0/>).

1. Introduction

Forest ecosystems are sensitive to climate variations and are crucial for ecological services, notably for carbon sequestration [1,2]. Of the estimated 2.19×10^{18} kg of carbon in the total biosphere carbon pool, a significant portion, approximately 1.0×10^{18} kg, is sequestered in forest ecosystems, which hold about 50% more carbon than the current atmospheric pool [3]. Predictions suggest a mean global temperature rise of 0.3–1.7 °C to 2.6–4.8 °C by 2100, posing significant challenges to these ecosystems, including potential productivity decline, biodiversity loss, and forest degradation [4–7]. Trees mitigate varied responses to global warming [8–10]. Although studies have shown that warming may limit habitats for species like *Nothofagus pumilio* (Poepf. & Endl.) Krasser (Nothofagaceae) [8] and *Picea mariana* (Mill.) Britton, Sterns & Poggenb. (Pinaceae) [9], it could benefit tree growth

in temperate and boreal regions [10]. This variability in tree responses to climate change highlights the importance of adaptive management and conservation in forest ecosystems.

Researchers have utilized statistical models, species distribution data, and environmental variables to simulate potential future distributions of forest ecosystems under climate change [11–13]. The Maximum Entropy Model (Maxent), integrating machine learning with maximum entropy principles, effectively predicts species' potential distributions by utilizing known geographical data and environmental factors [14]. Elith et al. [15] compared Maxent's accuracy and consistency against 16 species distribution models across 226 species and found it superior in performance and stability across varied sample sizes. Maxent's low bias, high data tolerance, and effectiveness with small samples make it a preferred choice for predicting species spatial distribution, especially for tree species [16]. For instance, Carlos et al. [11] demonstrated Maxent's high predictive accuracy and stability for 17 economically significant Mexican pine species, where it outperformed nine other models, which highlights its potential for modeling tree species distribution.

However, Maxent has several limitations, including the need for high-quality data, appropriate environmental variables, optimal parameters, and uncertainty assessment [17,18]. Using the default or a priori parameters and including all environmental variables can complicate the model and limit its application and accuracy, resulting in a decrease in the capacity of species translocation [19,20]. Moreover, the Intergovernmental Panel on Climate Change (IPCC) has updated the future climate scenarios, requiring more in-depth simulation analysis [4]. The WorldClim database (<http://worldclim.org>, in its 2020 update to version 2.1, extended the period of historical climate data from the 1960s–1990s to include the 1970s–2000s [21]. This update marked a significant shift from the Representative Concentration Pathways (RCPs) used for the IPCC's Fifth Coupled Model Intercomparison Project (CMIP5) to the Shared Socioeconomic Pathways (SSPs) of the CMIP6 framework. The SSPs in version 2.1 provided granular future climate projections: SSP1-2.6 (Sustainability) targeted a warming scenario substantially below 1.5 °C by 2100; SSP2-4.5 (Middle of the Road) projected a radiative force of approximately 4.5 W/m² by 2100; SSP3-7.0 (Regional Rivalry) indicated scenarios of high social fragility coupled with a significant anthropogenic radiative force; and SSP5-8.5 (Fossil-fueled Development) forecast the most extreme scenario, with radiative force reaching 8.5 W/m² by 2100 [4,22,23]. These SSPs enhanced our understanding of the interplay between socioeconomic development and climate change, resulting in more precise and realistic climate simulations [24]. Hence, the meticulous choice of environmental factors and model parameters is crucial for effective Maxent applications.

Research on tree habitats often focuses on single species, whereas few comprehensive studies have been conducted on different species, such as conifer and broadleaf trees. Therefore, there is limited understanding of their growth suitability and response to climate change, which will affect forest management. Climate warming has affected the geographic distribution and growth patterns of coniferous and broadleaf trees in northeast China [25–27]. Research by Lyu et al. [28] on *Pinus koraiensis* Siebold & Zucc. (Pinaceae) and *Quercus mongolica* Fisch. ex Ledeb. (Fagaceae) in this region revealed that the radial growth of *Quercus mongolica* is predominantly precipitation-dependent during the growing season, while *Pinus koraiensis* growth is more temperature-sensitive. Located in the Greater Khingan Range, the forests in the northern region of northeast China not only represent 29.9% of the country's natural forests but also encompass one-third of the carbon stock within China's forest ecosystems [29,30]. Notably, since 1961, the Greater Khingan Range has exhibited a significant warming trend, with its annual average temperature increase reaching 0.88 °C, far exceeding the national average rate of 0.02 °C [31]. This pronounced climate change has made the Greater Khingan Range an ideal location for studying the responses and adaptive mechanisms of trees to global warming.

Against this backdrop, two key species in the Greater Khingan Range forests, *Larix gmelinii* (Rupr.) Kuzen. (Pinaceae) and *Quercus mongolica* Fisch. ex Ledeb. (Fagaceae) have become focal points of study. These species are critical indicators of climate change and play vital roles in their respective forest ecosystems [27]. They exhibit a complex coexistence

with other species, such as *Pinus koraiensis* Siebold & Zucc. (Pinaceae) and *Betula platyphylla* Sukaczew (Betulaceae), forming diverse inter-species relationships [32–34]. *Larix gmelinii*, known for its cold tolerance and drought resistance, is one of the dominant vegetation species in the northern part of China's cold temperate coniferous forest zone [35]. It accounts for over 70% of the forest coverage in the Greater Khingan Range [36], and its carbon storage represents approximately 8.5% of the total forest carbon reserves in China [37]. This species plays a crucial role in maintaining the ecological balance in the northeast region of the country [38]. *Quercus mongolica*, as one of the most important deciduous tree species in northeast China, is classified as a secondary precious tree species. It is characterized by rapid growth and high-quality timber [39] and exhibits significant biomass accumulation and productivity in temperate zones. The ecosystem biocycling capacity of *Quercus mongolica* forests not only surpasses that of subtropical *Cunninghamia lanceolata* (Lamb.) Hook. (Cupressaceae) mature forests but also exceeds that of common pioneer tree species in temperate regions, such as *Betula platyphylla* [39–44].

To address this research gap, we employed a Maxent model optimized with the kuenm R package (<https://github.com/marloncobos/kuenm>, accessed on 2 January 2023) to predict the future distributions of *Larix gmelinii* and *Quercus mongolica* in the Greater Khingan Range. Leveraging updated IPCC data [21], we aimed to assess the impact of future climate change on these species in detail. Our study focuses on (1) defining the species' current and future distributions and suitabilities under various climate scenarios and (2) comparing the distributions, trends, and mechanisms of these species. We hypothesize a northward shift under future climate change and expect *Larix gmelinii* to be more sensitive to these changes than *Quercus mongolica*.

This study utilized a Maxent model optimized with R language to investigate the diverse responses and adaptation strategies of coniferous and broadleaf species to climate change, thereby contributing to a deeper understanding of forest–climate interactions. This research lays a scientific foundation for the conservation of the Greater Khingan Range's forest ecosystem. Additionally, the integration of Geographic Information System (GIS) methods with the Maxent model demonstrates the practical application value of this methodological combination in ecological protection and management.

2. Materials and Method

2.1. Collection of Species Occurrence Data

The occurrence data of *Larix gmelinii* and *Quercus mongolica* were obtained from two primary sources: (1) extensive field surveys by our research team in the Greater Khingan Range between 2019 and 2023 to map the species distribution comprehensively and (2) digitized historical specimen data from the Global Biodiversity Information Facility (GBIF; <http://www.gbif.org>) and the National Plant Specimen Resource Center (NSII; <http://www.cvh.ac.cn>), which provided essential historical insights into the species' distributions.

To ensure data accuracy and minimize spatial autocorrelation, we carefully screened records for precise latitude and longitude information, retaining only one record within a 1 km radius to avoid redundancy [45,46]. This strategy resulted in a robust dataset of 186 and 127 unique, spatially distinct occurrence records for *Larix gmelinii* and *Quercus mongolica*, respectively, serving as the basis for niche modeling and predicting potential future distributions under various climate scenarios (Figure 1).

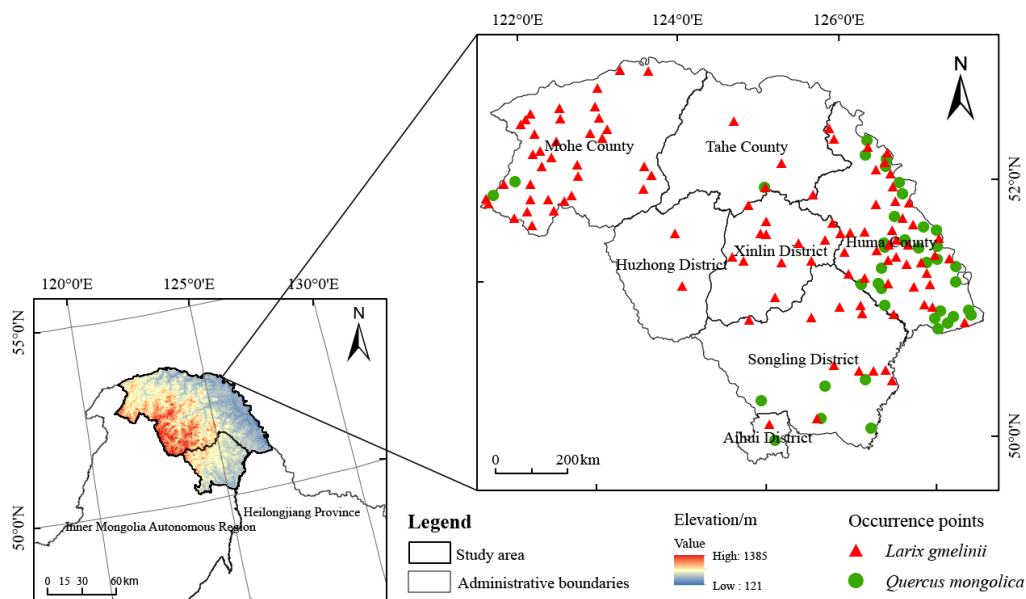


Figure 1. Administrative borders and research zone (left) alongside Greater Khinggan Prefecture (areas surveyed) featuring the presence data of *Larix gmelinii* and *Quercus mongolica* (right).

2.2. Environmental Data Acquisition and Processing

We integrated topographical, soil, and 19 bioclimatic variables (Tables 1 and A1). The bioclimatic variables were derived from the WorldClim database (<http://worldclim.org>), and Shared Socioeconomic Pathways (SSPs) from the Sixth Coupled Model Intercomparison Project (CMIP6) were used to project future scenarios (2050s and 2070s) under three climate scenarios (SSP1-2.6, SSP2-4.5, and SSP5-8.5) at a 30-arc-second resolution [47,48]. These climate data, generated by the Beijing Climate Center's Medium-Resolution Climate System Model (BCC.CSM2.MR), are noted for their accuracy at simulating China's precipitation and temperature patterns [49,50]. Soil data came from the World Soil Database (<http://www.fao.org>), and topographic data (high-resolution (90 m) elevation data) were sourced from the Chinese Academy of Sciences' Resource and Environmental Science Data Center (<http://www.resdc.cn/>). The vector zoning map of the study area was sourced from the National Administration of Surveying, Mapping and Geoinformation's standard map service website (<http://bzdt.ch.mnr.gov.cn/>).

The Maxent model necessitates that the environmental data inputs must rigorously maintain uniform spatial reference coordinates and resolution. Accordingly, the vector map of the study area is utilized as a boundary, and the ArcGIS (Version 10.4, ESRI, Redland, CA, USA) mask tool is employed for batch extraction of the pertinent environmental variable layers. Additionally, the resampling tool under raster processing is utilized to standardize the spatial resolution: that is, the pixel size (X, Y) of the environmental layers. Subsequently, utilizing the 'From Raster to ASCII' functionality in ArcGIS, the datasets containing environmental variables were converted into ASCII format.

2.3. Model

The complexity of the model constitutes a critical aspect in the investigation of species distribution models. An effective model must strike a balance between accurately fitting the data and constraining overly complex functional relationships [51]. Maxent, as an algorithmic model, is inclined to form complex functional relationships to align with observational data. This tendency significantly contributes to the model's enhanced predictive capabilities: a notable strength of the maximum entropy approach [52].

The complexity of the Maxent model is primarily influenced by three factors: the number of environmental variables included, the types of functional modes (or 'features') used, and the regularization multiplier [53,54].

The choice of environmental variables is pivotal; an excess can lead to computational inefficiencies and challenges in interpreting the results, especially when variables display high collinearity [19,51]. Therefore, a balanced approach for selecting these variables is crucial for both computational efficiency and clarity of interpretation.

Regularization plays a vital role in Maxent by constraining variable weights, ensuring a balance between model fit and extrapolation. This prevents overfitting, allowing the model to maintain a margin of error [55]. Maxent's versatility is further illustrated by its six functional modes: linear (L), quadratic (Q), product (P), threshold (T), hinge (H), and category (C), each catering to different variable interactions and types [56,57]. Maxent dynamically tests combinations of these modes, ultimately selecting the one that achieves the highest Area Under the Curve (AUC) for prediction.

Model performance is critically evaluated using the AUC, a metric derived from the Receiver Operating Characteristic (ROC) curve [14]. The ROC curve is a plot of the false positive rate against the true positive rate at various thresholds [14]. The AUC, measuring the area under this curve, provides a robust measure of model performance and is applicable across various thresholds [58]. Its range from 0 to 1, with values nearer to 1 reflecting greater predictive accuracy, classifies performance into four categories [59,60]: poor (0.6–0.7), fair (0.7–0.8), good (0.8–0.9), and excellent (0.9–1).

2.3.1. Environmental Variable Selection

Considering the potentially high correlations among 19 bioclimate variables, such multicollinearity could lead to data overfitting when these factors are directly used in model construction using the Maxent software (v3.4.4, Biodiversity Informatics, Cambridge, MA, USA), thereby affecting the simulation results [61]. Pearson correlation analysis was conducted by the software ENMTools v1.3 [62,63] to refine our variable selection; we focused on factors with a correlation coefficient above 0.8 (Figure A1). Utilizing Maxent 3.4.4, ten calculations were performed on the selected environmental variables to establish an initial model. Based on the average results of these ten computations, environmental factors with a contribution rate of less than 1% were excluded. This selection process was guided by a comprehensive consideration of the species' environmental needs and physiological traits, resulting in the identification of key variables for modeling (Table 1).

Table 1. Environmental variables considered in the Maxent models of *Larix gmelinii* and *Quercus mongolica* in the Greater Khingan Range.

Variable Types	Code and Unit	Species	
		<i>Larix gmelinii</i>	<i>Quercus mongolica</i>
Annual Mean Temperature	BIO1 (°C)	–	✓
Isothermality × 100	BIO3 (°C)	✓	✓
Mean Temperature of Warmest Quarter	BIO10 (°C)	✓	✓
Mean Temperature of Coldest Quarter	BIO11 (°C)	✓	–
Annual Precipitation	BIO12 (mm)	✓	–
Precipitation Seasonality (Co-efficient of Variation)	BIO15 (mm)	✓	–
Precipitation of Driest Quarter	BIO17 (mm)	✓	–
Soil Total Organic Carbon Content	T_CACO3 (%)	✓	✓
Total Organic Carbon Content	T_OC (%)	–	✓
Soil Base Saturation	S_BS (%)	✓	–
Elevation	Elevation (m)	✓	✓
Slope	Slope (degree)	–	✓
Aspect	Aspect (degree)	–	✓

The variables marked with “✓” are used for building the model.

2.3.2. Model Calibration

Model calibration is a process in which the aim is to determine which combination of parameters best represents the phenomenon of interest by finding the best fit with the data [64]. Performed manually, detailed model calibration and final model creation is

quite time-consuming (e.g., a week or more). Hence, automating the process is essential for increasing the robustness of Ecological Niche Models (ENMs) [54]. Here, we employed *kuenm*, an R package that automates important calibration and evaluation steps in ENM. In its current version, this package uses Maxent as the modeling algorithm and automates model calibration and the creation of final models [54]. For each species, we created 1240 candidate models by combining 3 sets of environmental variables, 40 values of regularization multipliers (RMs, 0.1–4 at intervals of 0.1), and all 31 possible combinations of 5 feature classes (FCs). The R software (Version 4.1.1, R Foundation for Statistical Computing, Vienna, Austria) evaluates candidate model performance and initially selects statistically significant models with omission rates $\leq 5\%$ [54]. Subsequently, models with a Delta-corrected Akaike Information Criterion (AICc) of ≤ 2 are chosen [17,51,54].

2.3.3. Threshold Determination

After determining the best configuration of the FC and RM, we reserved 25% of the samples for testing. The significance of the environmental variables was evaluated through jackknife tests, which were conducted ten times to ensure robustness. The mean values of the iterations were used as predictive results. Utilizing the ArcGIS software (Version 10.4, ESRI, Redland, CA, USA) (specifically, the ArcToolbox: Conversion Tools), the species distribution maps generated by the Maxent model (.asc files) were converted into raster data (.tif files), resulting in suitability maps that represented the probability of species occurrence ($0 < p \leq 1$).

We adopted the maximum test sensitivity plus specificity (MTSPS) threshold as a criterion to delineate suitable and unsuitable areas to effectively consider both omission and commission errors [65–67]. Suitable habitat was further categorized into three levels: low (MTSPS $< p \leq 0.4$), moderate ($0.4 < p \leq 0.6$), and high suitability ($p > 0.6$) [68].

2.4. Habitat Change Analysis and Centroid Shifts

To ensure the temporal comparability of Maxent, we maintained the consistency of topographical and soil variables while focusing exclusively on changes to bioclimatic variables to predict future spatial patterns of species distribution [69,70]. Additionally, we cited a hypothesis that species possess unrestricted migration capacities when evaluating the impact of future climatic changes on species distribution [71]. This implies that in response to climatic alterations, species may either adapt and persist in their current habitats, potentially relocate to newly viable regions, or face in situ extinction. Based on this hypothesis, we categorized the changes in the species' potential habitats into four types (expansion, unsuitable, no change, and contraction) based on future area changes relative to the current suitable habitats. In the habitat change matrix, transitions from 0 to 1 indicated expansion, 1 to 0 contraction, 1 to 1 persistence, and 0 to 0 consistent unsuitability. Finally, to compare the responses of the geographical suitability areas of *Larix gmelinii* and *Quercus mongolica* under various future climate scenarios, we implemented the following steps: initially, the raster data were reclassified; subsequently, a raster calculator was utilized to determine the expansion or contraction of the suitable habitat ranges for both tree species under different future climate scenarios.

Due to the irregular boundaries of habitats, the centroids of the species records in the entire geographic range were determined to assess the changes between current and future conditions. We used SDMtoolbox 2.4 to assess the trends of the centroid shifts between adjacent habitat stages and calculated the centroid migration distances [46].

3. Results

3.1. Model Performance

Automatic analysis using the R program indicated that all 1240 candidate models were statistically significant. One recommended model was selected for each species (Figure 2); both had a DeltaAICc value of 0. This result indicated optimal model transferability from known to predicted distribution areas and the avoidance of overfitting; thus, these were

the best models. The FC was Q, P, and T for *Larix gmelinii* and H for *Quercus mongolica*. The RM values were 1.7 for *Larix gmelinii* and 1 for *Quercus mongolica*. For these optimal FC and RM settings, the AUC values of the Maxent prediction results were 0.921 for *Larix gmelinii* and 0.985 for *Quercus mongolica* (Figure 3).

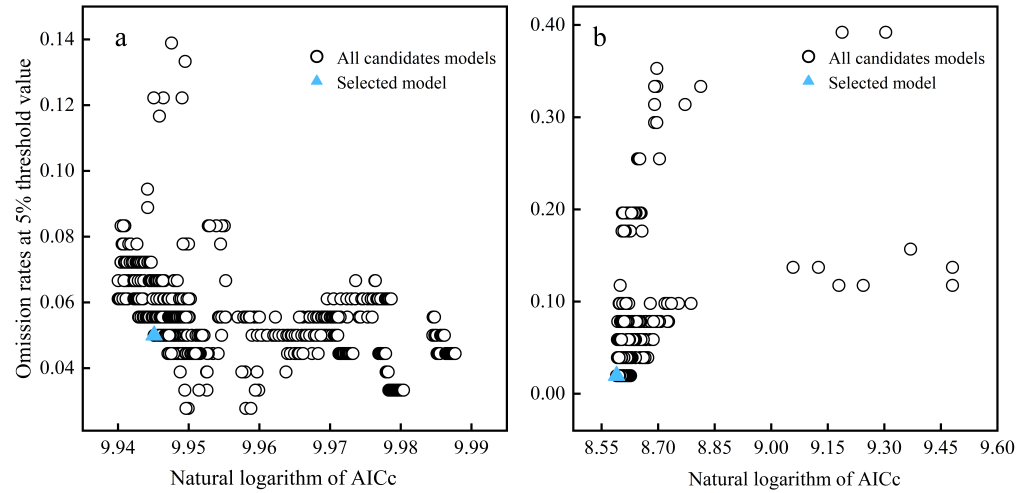


Figure 2. Omission rates and AICc values for *Larix gmelinii* (a) and *Quercus mongolica* (b), including all candidate models and the chosen ‘best’ models.

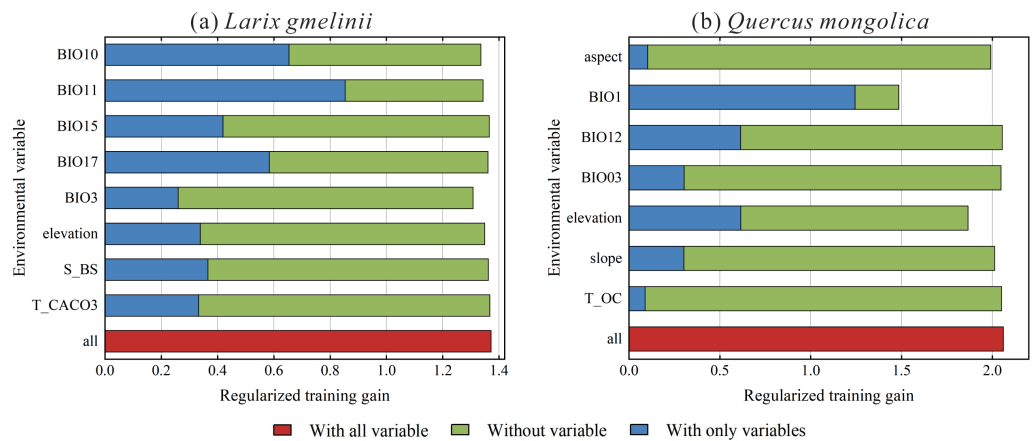


Figure 3. The outcomes of the jackknife test elucidate the significance of various variables for the habitat distribution modeling of (a) *Larix gmelinii* and (b) *Quercus mongolica*. The regularized training gain quantifies the enhancement in the Maxent model’s fit to the existing data, as opposed to a uniform distribution. Dark blue bars represent the gain achieved by employing each variable independently for each species, light blue bars reflect the reduction in gain consequent to the exclusion of a single variable from the comprehensive model for each species, and the red bar denotes the gain attained with the incorporation of all variables for each species.

3.2. Variable Importance

Environmental variables crucial for *Larix gmelinii* and *Quercus mongolica* were identified through contribution rate analysis (Figure 4 and Table 2). For *Larix gmelinii*, BIO11, BIO10, and BIO17 accounted for 71.6% of the model’s predictive power, underlining their critical role in determining its potential geographic distribution. In contrast, for *Quercus mongolica*, BIO1, elevation, and BIO12 contributed 90%, dominating the model and shaping the species’ current potentially suitable habitat.

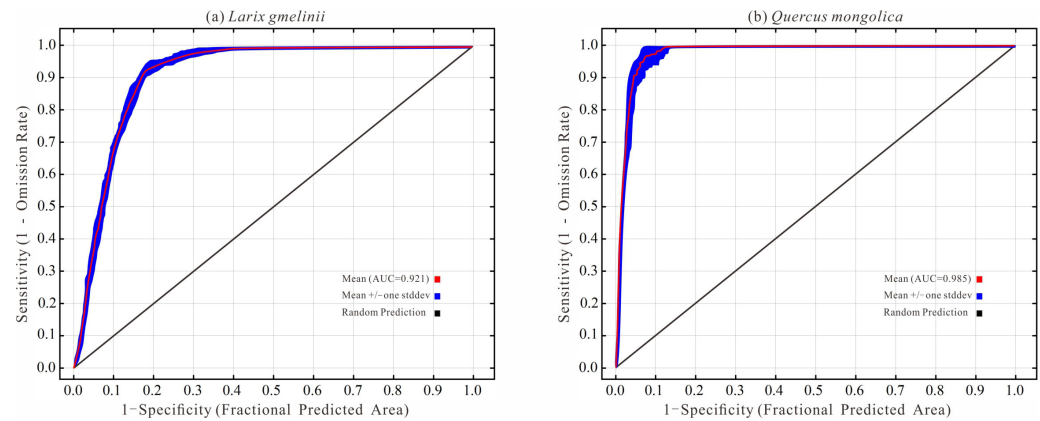


Figure 4. AUC curve representation: (a) *Larix gmelinii* and (b) *Quercus mongolica* distribution model development. The red curve represents the training data, indicating model alignment with the training dataset; the blue curve represents the testing data, reflecting the model's predictive performance in practical tests.

Table 2. Contribution rate of environmental variable importance obtained by jackknife test.

Species	Variable	Percent Contribution (%)
<i>Larix gmelinii</i>	BIO11	37.1
	BIO10	19.5
	BIO17	15
	T_CACO3	11.4
	BIO3	5.9
	S_BS	5.3
	BIO15	3.3
	elevation	2.6
<i>Quercus mongolica</i>	BIO1	64.4
	elevation	21.1
	BIO12	4.8
	slope	4.2
	aspect	3.1
	BIO3	1.1
	T_OC	1

The red lines in Figure 5 display the influence of individual environmental factors on the predicted probability of occurrence. Details on other environmental factors can be found in Figures A2 and A4. Specifically, Figure 5a illustrates that the occurrence probability for *Larix gmelinii* increases as BIO11 and BIO10 decrease: peaking before stabilizing and forming a response crest. This finding reveals that *Larix gmelinii* consistently reacts to temperature variations, implying a decline in its suitable habitat as temperatures increase. Conversely, BIO17 shows a positive correlation with the distribution probability. As BIO17 increases, the logistical probability value rises and remains consistently high. For *Quercus mongolica*, elevation and BIO1 stabilize at high probabilities at fixed thresholds but decrease with increasing variable values and then stabilize. The relationship between BIO12 and the distribution probability differs slightly, with a minor increase in probability as annual precipitation rises, followed by stabilization. Most precipitation values correspond to high probability levels, indicating a comparatively lower contribution and importance of annual precipitation to the distribution probability prediction for *Quercus mongolica* relative to the other two dominant factors.

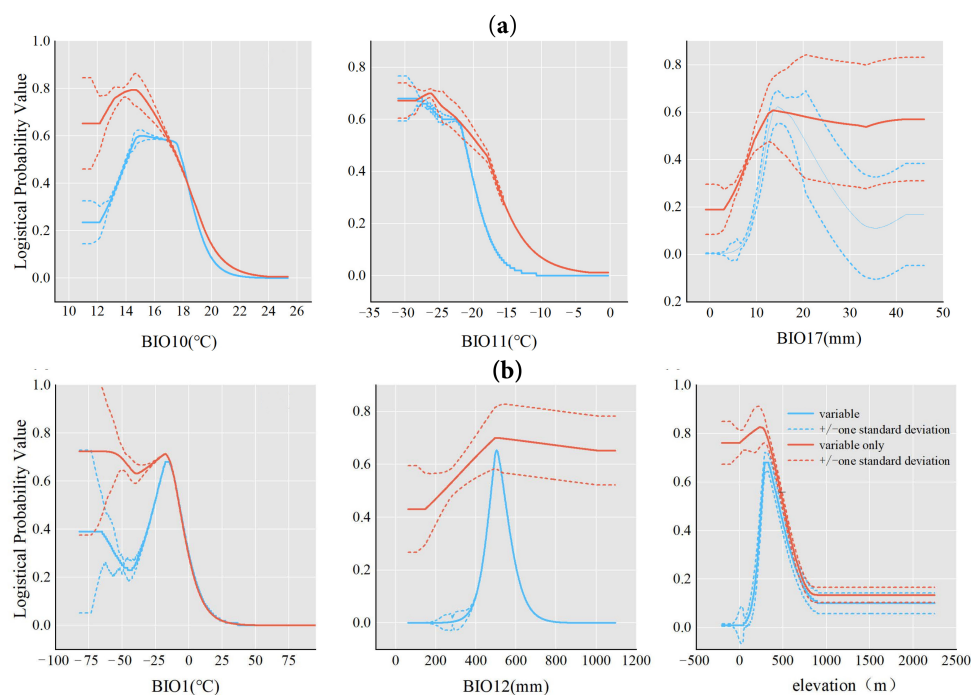


Figure 5. Response curves characterizing how dominant variables affected the Maxent predictions for *Larix gmelinii* (a) and *Quercus mongolica* (b). Red lines represent logistical predictions varying with each climatic variable while holding other variables at their means. Based on individual variables, the Maxent models generate blue lines. Solid lines show the average of ten Maxent runs, and dashed lines denote one standard deviation from this mean.

The blue lines in Figure 5 display the distinct effects of the key variables in the optimal model on forecasting the likelihood of favorable conditions, as demonstrated by a Maxent model that incorporates each variable independently. Details on other environmental factors can be found in Figures A3 and A5. *Larix gmelinii*'s occurrence probability approaches zero with BIO11 above -10°C , increases sharply as temperatures decrease, and peaks below -28°C . This result suggests a stringent upper limit but no lower limit for BIO11. The suitable distribution for *Larix gmelinii* (probability ≥ 0.24) requires that BIO11 is below -19°C . In contrast to BIO11, BIO10 and BIO17 have upper and lower limits. The probability approaches zero for BIO17 below 7 mm, rapidly increases to its highest level at 14 mm, and sharply declines above this value. Similarly, the probability of BIO10 stabilizes around 0.23 when temperatures are below 12°C and increases with rising temperatures, maintaining high levels between 15°C and 17°C , followed by a downward trend. The suitable distribution area for *Larix gmelinii* requires BIO10 and BIO17 ranges of $12\text{--}19^{\circ}\text{C}$ and $10\text{--}28\text{ mm}$, respectively. The occurrence probability of *Quercus mongolica* approaches zero when BIO01 exceeds 18°C , with the optimal BIO1 range of -20°C to -10°C . Unlike temperature, precipitation and elevation require stringent thresholds. The occurrence probability approaches zero when the elevation is below 140 m and BIO12 is below 400 mm. This probability surges with increasing values, peaking at 340 m for elevation and 505 mm for BIO12 before sharply decreasing beyond these points. The suitable distribution for *Quercus mongolica* (probability ≥ 0.15) necessitates an elevation range of $166\text{--}776\text{ m}$ and annual precipitation of $415\text{--}620\text{ mm}$.

3.3. Potential Current and Future Habitat Distributions

3.3.1. *Larix gmelinii*

Under the current climate, the unsuitable habitat area for *Larix gmelinii* accounts for only 2.06% of the research zone, whereas the suitable habitat encompasses a significant 98.02%, demonstrating its high adaptability to current climate conditions (Figure 6 and

Table 3). Within the suitable habitat, marginally suitable, moderately suitable, and highly suitable habitats comprise 14.17%, 37.33%, and 46.52%, respectively, indicating that most areas offer ideal conditions for *Larix gmelinii*. Future climate shifts, however, are expected to alter these habitats (Figure 7 and Table 3). By the 2050s, various climate scenarios predict an expansion of unsuitable habitats: notably, to 29.02% under the SSP5-8.5 scenario. However, the conditions will differ by the 2070s. Under SSP1-2.6, suitable habitats will revert to near-current levels at 98.43%, whereas under the SSP2-4.5 and SSP5-8.5 scenarios, unsuitable areas could expand to 17.65% and 54.06%, respectively. In particular, a substantial increase in unsuitable habitats is observed in the SSP5-8.5 scenario, potentially covering over half of the study area. These results highlight the notable influence of varying climate scenarios on the suitable habitat of *Larix gmelinii* and the looming threat of climate change to its distribution. Additionally, the shift in suitability zones is noteworthy. Under most climate scenarios, moderately and highly suitable habitats for *Larix gmelinii* decrease, whereas marginally suitable areas increase, hinting at a potential overall decline in future growth conditions. These effects are especially pronounced in the SSP5-8.5 scenario, where highly suitable habitats will shrink to 3.66% by the 2070s—much lower than in other scenarios—suggesting a scarcity of optimal growth environments under extreme climate conditions.

Table 3. Forecast areas unsuitable and suitable for *Larix gmelinii* under current and future climate scenarios.

SSPs (Year)	Unsuitable Habitats	Total Suitable Habitats	Minimally Suitable Habitats	Moderately Suitable Habitats	Highly Suitable Habitats
	Area /km ² (%)	Area/km ² (%)	Area /km ² (%)	Area /km ² (%)	Area /km ² (%)
Current	1701.8 2.06	81,104.7 98.02	11,724.9 14.17	30,885.3 37.33	38,494.5 46.52
SSP1-2.6 (2050s)	6142.0 7.42	76,687.9 92.68	7138.4 8.63	24,326.6 29.40	45,222.9 54.65
SSP2-4.5 (2050s)	12,183.3 14.72	70,646.6 85.38	9965.7 12.04	18,502.4 22.36	42,178.5 50.97
SSP5-8.5 (2050s)	24012.2 29.02	58817.7 71.08	11,972.8 14.47	42,373.2 51.21	4471.7 5.40
SSP1-2.6 (2070s)	1360.0 1.64	81,446.6 98.43	3656.6 4.42	22,681.3 27.41	55,108.7 66.60
SSP2-4.5 (2070s)	14,602.1 17.65	68,227.8 82.46	12,050.2 14.56	34,774.7 42.03	21,402.8 25.87
SSP5-8.5 (2070s)	44,732.1 54.06	38,097.7 46.04	24,590.3 29.72	10,480.6 12.67	3026.9 3.66

SSPs: Shared Socioeconomic Pathways; SSP1-2.6: Sustainable Development Pathway; SSP2-4.5: Moderate Development Pathway; SSP5-8.5: Conventional Development Pathway Dominated by Fossil Fuels. The proportion of suitable habitat area under different future climate scenarios is the average for the periods 2021–2040, 2041–2060, and 2061–2080.

In summary, future climate change will significantly affect the habitats of *Larix gmelinii*, with diverse impacts under different climate scenarios. These findings not only underline potential risks to this species but also emphasize the diverse responses for different levels of suitable habitats.

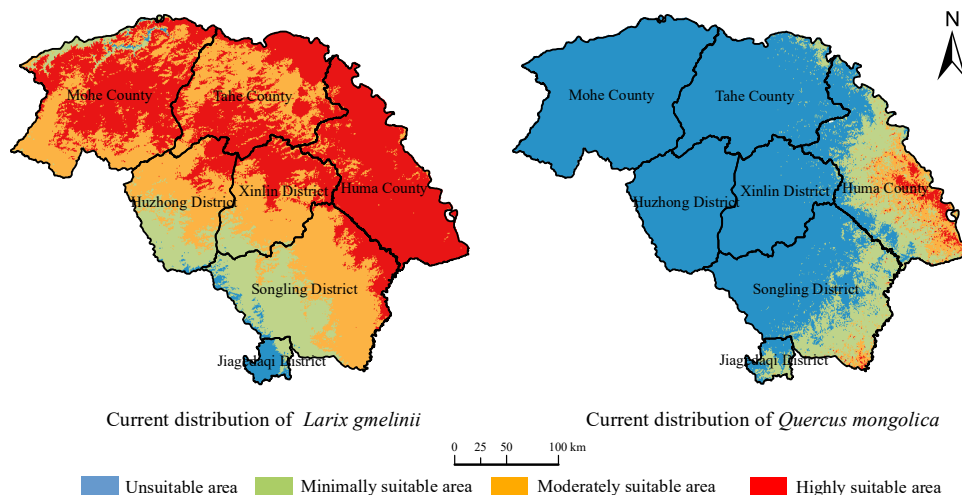


Figure 6. Suitable habitat distribution of *Larix gmelinii* (left) and *Quercus mongolica* (right) in the Greater Khingan Range under current climatic conditions.

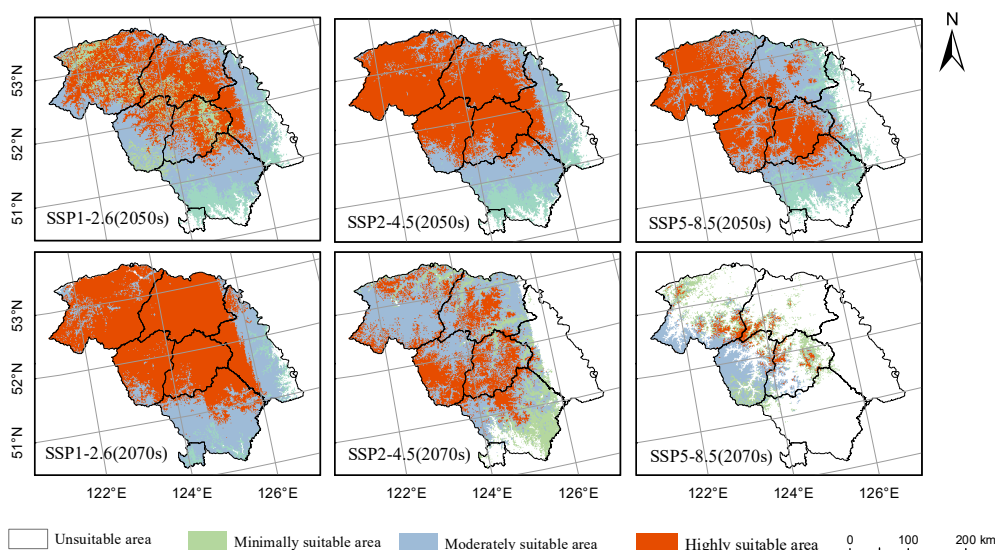


Figure 7. Future distribution of *Larix gmelinii* as a reaction to future climate change scenarios during 2050s and 2070s. SSPs: Shared Socioeconomic Pathways; SSP1-2.6: Sustainable Development Pathway; SSP2-4.5: Moderate Development Pathway; SSP5-8.5: Conventional Development Pathway Dominated by Fossil Fuels.

3.3.2. *Quercus mongolica*

Currently, 79.64% of the study area is unsuitable for *Quercus mongolica*; only 20.36% is suitable (Figure 6 and Table 4). Future climate scenarios predict a significant increase in suitable habitat (Figure 8 and Table 4). Suitable habitat will comprise the majority by the 2050s under the SSP1-2.6, SSP2-4.5, and SSP5-8.5 scenarios (66.28%, 78.39%, and 89.09%, respectively). This expansion intensifies by the 2070s, particularly under SSP5-8.5, with suitable habitats nearly encompassing the whole area (99.99%). A key trend in this shift is the marked rise in marginally suitable habitats; they will account for 67.84% under SSP5-8.5 by the 2050s, increasing to 95.42% by the 2070s. Meanwhile, moderately suitable habitats will exhibit relatively minor changes.

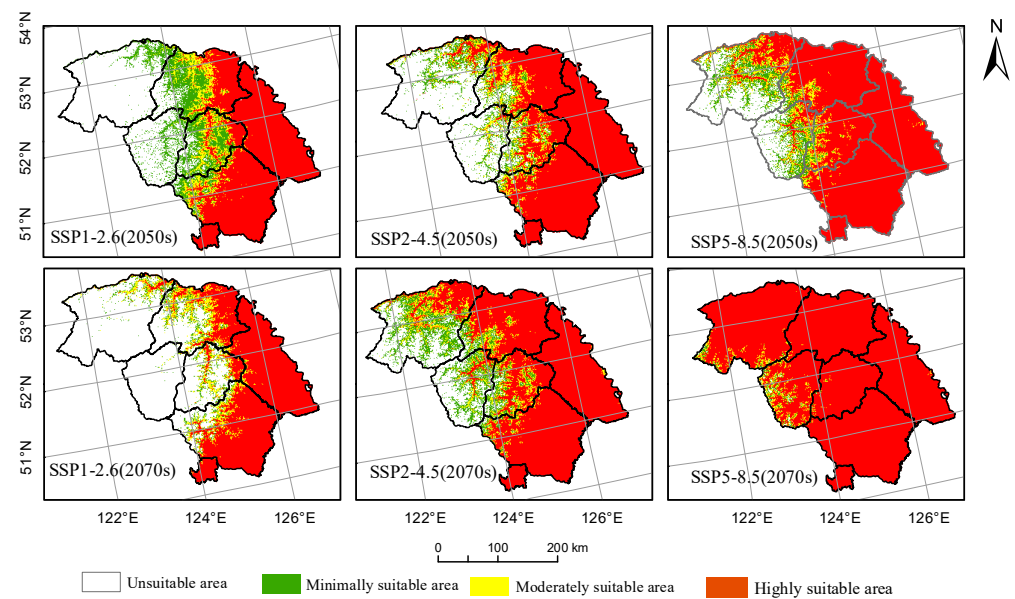


Figure 8. Future distribution of *Quercus mongolica* as a reaction to future climate change scenarios during 2050s and 2070s. SSPs: Shared Socioeconomic Pathways; SSP1-2.6: Sustainable Development Pathway; SSP2-4.5: Moderate Development Pathway; SSP5-8.5: Conventional Development Pathway Dominated by Fossil Fuels.

Table 4. Forecast areas unsuitable and suitable for *Quercus mongolica* under current and future climate scenarios.

SSPs (Year)	Unsuitable Habitats	Total Suitable Habitats	Minimally Suitable Habitats	Moderately Suitable Habitats	Highly Suitable Habitats
	Area /km ² (%)	Area/km ² (%)	Area /km ² (%)	Area /km ² (%)	Area /km ² (%)
Current	65,896.4 79.64	16,848.4 20.36	11,967.0 14.46	3745.5 4.53	1135.9 1.37
SSP1-2.6 (2050s)	27,897.9 33.72	54,846.9 66.28	12,473.4 15.07	6610.1 7.99	35,763.4 43.22
SSP2-4.5 (2050s)	17,958.6 21.70	64,866.1 78.39	12,156.8 14.69	6658.5 8.05	46,050.8 55.65
SSP5-8.5 (2050s)	9111.2 11.01	73,713.5 89.09	10,446.4 12.62	7137.0 8.63	56,130.1 67.84
SSP1-2.6 (2070s)	29,908.1 36.14	52,916.6 63.95	12,642.7 15.28	6660.7 8.05	33,613.3 40.62
SSP2-4.5 (2070s)	8058.2 9.74	74,766.6 90.36	15,597.5 18.85	7757.7 9.38	51,411.4 62.13
SSP5-8.5 (2070s)	86.5 0.10	82,738.2 99.99	1220.2 1.47	2564.9 3.10	78,953.2 95.42

SSPs: Shared Socioeconomic Pathways; SSP1-2.6: Sustainable Development Pathway; SSP2-4.5: Moderate Development Pathway; SSP5-8.5: Conventional Development Pathway Dominated by Fossil Fuels; The proportion of suitable habitat area under different future climate scenarios is the average for the periods 2021–2040, 2041–2060, and 2061–2080.

These data reveal that *Quercus mongolica*'s habitat will change significantly under different future climate scenarios. Generally, its suitable habitat will expand, especially under extreme scenarios, potentially covering the entire study area. However, the majority

of this expanded habitat will fall into the low suitability category, suggesting that the quality of its habitat could diminish although the species may extend its range.

3.4. Differences in the Distribution of Current and Future Habitats

3.4.1. *Larix gmelinii*

The results from the Maxent model showed a shift in the habitat distributions of *Larix gmelinii* over time (Figure 9 and Table 5). The largest no-change area regarding suitability is 75,766.29 km² by the 2050s under the SSP1-2.6 scenario. In contrast, the SSP5-8.5 scenario predicts the most extensive contraction of suitable areas (23,202.01 km²). The ability of the species to adapt will be more complex by the 2070s. The large, stable area of 79,760.56 km² expands by 1686.04 km² under SSP1-2.6, indicating resilience. In contrast, the suitable area sharply declines to 43,317.24 km² under the more extreme SSP5-8.5 scenario, nearly doubling the reduction observed in the 2050s and suggesting survival challenges. Interestingly, the stability of the unsuitable area at 687.06 km² under the 70s SSP2-4.5 scenario marks a significant shift from its decrease in the 2050s, indicating evolving habitat dynamics for *Larix gmelinii* over time, even for the same climate scenario.

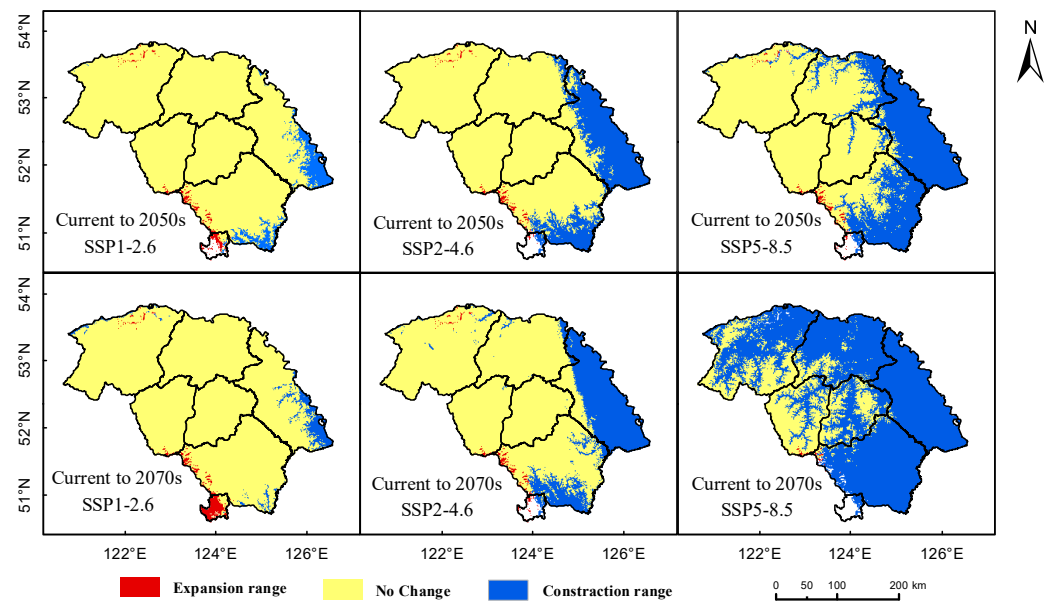


Figure 9. Future distribution of *Larix gmelinii* as a reaction to future climate change scenarios during 2050s and 2070s. SSPs: Shared Socioeconomic Pathways; SSP1-2.6: Sustainable Development Pathway; SSP2-4.5: Moderate Development Pathway; SSP5-8.5: Conventional Development Pathway Dominated by Fossil Fuels.

Table 5. Changes in the distribution of *Larix gmelinii*'s habitats comparing current to future climate change projections.

Current to SSPs (Year)	Expansion Range		Unsuitable		No Change		Contraction Range	
	Area (km ²)	%	Area (km ²)	%	Area (km ²)	%	Area (km ²)	%
SSP1-2.6 (2050s)	901.7	1.09	800.2	0.97	75,766.3	91.57	5338.4	6.45
SSP2-4.5 (2050s)	901.7	1.09	800.2	0.97	75,766.3	91.57	5338.4	6.45
SSP5-8.5 (2050s)	908.3	1.10	793.5	0.96	57,902.7	69.98	23,202.0	28.0
SSP1-2.6 (2070s)	1686.0	2.04	15.8	0.02	79,760.6	96.39	1344.2	1.62
SSP2-4.5 (2070s)	1014.8	1.23	687.1	0.83	67,194.7	81.21	13,910.1	16.81
SSP5-8.5 (2090s)	306.1	0.37	1395.7	1.69	37,787.5	45.67	43,317.2	52.35

SSPs: Shared Socioeconomic Pathways; SSP1-2.6: Sustainable Development Pathway; SSP2-4.5: Moderate Development Pathway; SSP5-8.5: Conventional Development Pathway Dominated by Fossil Fuels.

Overall, these findings indicate that *Larix gmelinii's* suitable habitat in the Greater Khingan Range is generally stable under future climate scenarios, but the species faces varying degrees of change and contraction risks.

3.4.2. *Quercus mongolica*

The evolving patterns of *Quercus mongolica's* habitat distributions exhibits notable characteristics (Figure 10 and Table 6). First, a stable suitable area of 16,916.15888 km² is consistent in all scenarios, indicating habitat stability. However, the degree of expansion differs. The areas of expansion are 47,941.181 km² and 56,754.02 km² in the 2050s under SSP2-4.5 and SSP5-8.5, respectively, surpassing the 37,933.05 m² under SSP1-2.6. A similar trend of larger expansions under SSP2-4.5 and SSP5-8.5 is observed in the 2070s. Second, the stable unsuitable areas show significant differences between the scenarios, especially under the 2070s SSP5-8.5 scenario, where it reduces to just 89.00 km². This finding suggests that *Quercus mongolica's* unsuitable areas might contract more under certain scenarios.

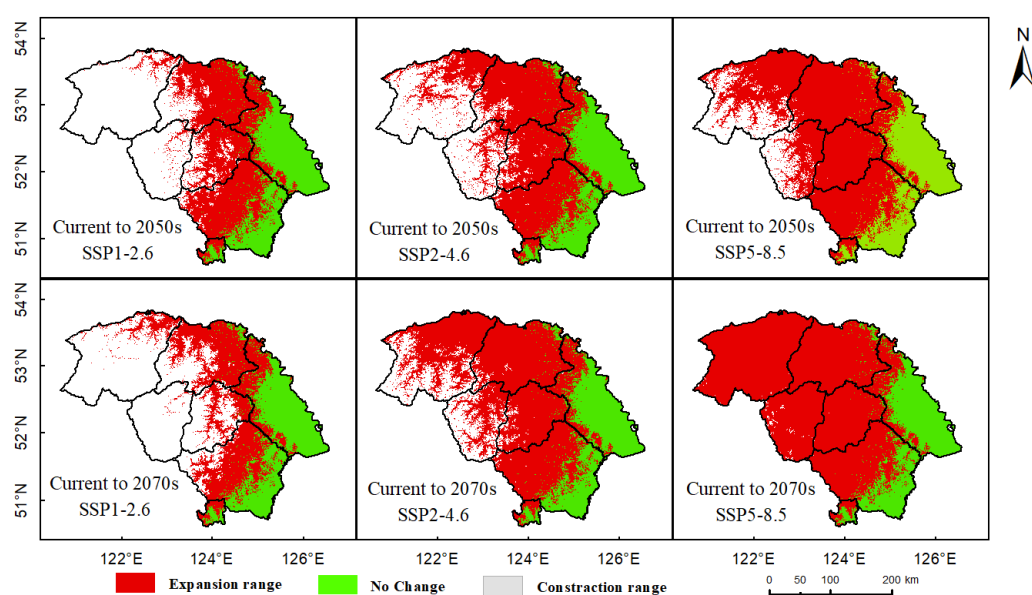


Figure 10. Changes in the distribution of *Quercus mongolica's* habitats comparing current to future climate change projections during 2050s and 2070s. SSPs: Shared Socioeconomic Pathways; SSP1-2.6: Sustainable Development Pathway; SSP2-4.5: Moderate Development Pathway; SSP5-8.5: Conventional Development Pathway Dominated by Fossil Fuels.

In summary, *Quercus mongolica's* future suitable habitat in the Greater Khingan Range is somewhat stable. However, the expansion and stability of the suitable and unsuitable areas differ markedly for different climate scenarios.

Table 6. Changes in the distribution of *Quercus mongolica's* habitats comparing current to future climate change projections.

Current to SSPs (year)	Expansion Range		Unsuitable		No Change		Contraction Range	
	Area (km ²)	%	Area (km ²)	%	Area (km ²)	%	Area (km ²)	%
SSP1-2.6 (2050s)	37,933.1	45.84	27,895.0	33.71	16,916.2	20.44	0.0	0.00
SSP2-4.5 (2050s)	47,941.2	57.94	17,886.9	21.62	16,916.2	20.44	0.0	0.00
SSP5-8.5 (2050s)	56,754.0	68.59	90,74.0	10.97	16,916.2	20.44	0.0	0.0
SSP1-2.6 (2070s)	35,924.3	43.42	29,903.8	36.14	16,916.2	20.44	0.0	0.00
SSP2-4.5 (2070s)	57,833.7	69.89	7994.4	9.66	16,916.2	20.44	0.0	0.00
SSP5-8.5 (2090s)	65,739.0	79.45	89.0	0.11	16,916.2	20.44	0.0	0.00

SSPs: Shared Socioeconomic Pathways; SSP1-2.6: Sustainable Development Pathway; SSP2-4.5: Moderate Development Pathway; SSP5-8.5: Conventional Development Pathway Dominated by Fossil Fuels.

3.5. Scope and Intensity of Distribution Shifts
 3.5.1. *Larix gmelinii*

The current geographic center for *Larix gmelinii* is located at 52.03° N, 124.33° E in Xinlin’s northwest (Figure 11 and Table 7). It will migrate to the northwest by the 2050s under different climate scenarios. Specifically, it migrates 8.45 km to 52.08° N and 124.24° E under SSP1-2.6. The shifts are more pronounced for SSP2-4.5 and SSP5-8.5 (30.3 km to 52.18° N, 123.97° E and 51.9 km to 52.27° N, 123.97° E, respectively).

Table 7. Predicted migration distances for *Larix gmelinii* and *Quercus mongolica* under different SSP scenarios.

Species	Initial Location (Lat, Long)	Scenario	Shifted Location (Lat, Long)	Migration Distance (km)
<i>Larix gmelinii</i>	52.03° N, 124.33° E	SSP1-2.6 (2050s)	52.08° N, 124.24° E	8.45
		SSP1-2.6 (2070s)	52.04° N, 124.28° E	5.67
		SSP2-4.5 (2050s)	52.18° N, 123.97° E	30.3
		SSP2-4.5 (2070s)	52.03° N, 124.32° E	1.19
		SSP5-8.5 (2050s)	52.27° N, 123.97° E	51.9
		SSP5-8.5 (2070s)	52.20° N, 123.35° E	25.3
<i>Quercus mongolica</i>	51.28° N, 125.83° E	SSP1-2.6 (2050s)	51.69° N, 125.18° E	64.2
		SSP1-2.6 (2070s)	51.73° N, 125.24° E	5.95
		SSP2-4.5 (2050s)	51.85° N, 124.87° E	92.24
		SSP2-4.5 (2070s)	51.95° N, 124.64° E	19.75
		SSP5-8.5 (2050s)	51.94° N, 124.64° E	110.6
		SSP5-8.5 (2070s)	52.01° N, 124.34° E	22.1

SSPs: Shared Socioeconomic Pathways; SSP1-2.6: Sustainable Development Pathway; SSP2-4.5: Moderate Development Pathway; SSP5-8.5: Conventional Development Pathway Dominated by Fossil Fuels.

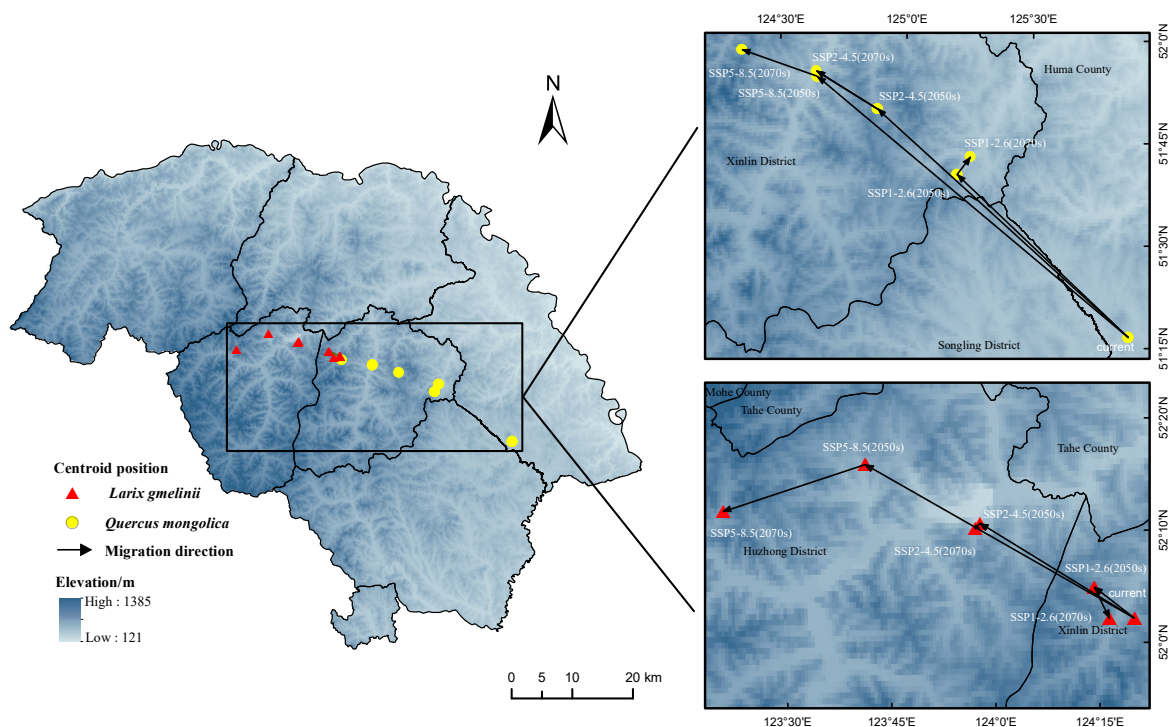


Figure 11. Location of the center of mass in the fitness zone of two tree species under different climate scenarios during 2050s and 2070s. SSPs: Shared Socioeconomic Pathways; SSP1-2.6: Sustainable Development Pathway; SSP2-4.5: Moderate Development Pathway; SSP5-8.5: Conventional Development Pathway Dominated by Fossil Fuels..

Larix gmelinii's centroid migrates southeast to 52.04° N, 124.28° E in the Xinlin District under SSP1-2.6, covering 5.67 km from the 2050s to the 2070s. It shifts a short distance southwest by 1.19 km under SSP2-4.5, indicating stability. In contrast, the shift is substantial under SSP5-8.5, and the centroid moves to 52.20° N, 123.35° E in the northwest Huzhong District, a distance of 25.3 km. These centroid movements reflect the nuanced climate impacts and adaptability challenges for *Larix gmelinii* in all scenarios.

3.5.2. *Quercus mongolica*

Currently, *Quercus mongolica*'s centroid is southwest of Huma County at 51.28° N, 125.83° E (Figure 11). Under SSP126, it migrates to the western Xinlin District by the 2050s (51.69° N, 125.18° E; 64.2 km) and shifts northeast by the 2070s (51.73° N, 125.24° E; 5.95 km). Under SSP245, the centroid migrates northwest to the northern Xinlin District by the 2050s (51.85° N, 124.87° E; 92.24 km) and continues northwest in the 2070s (51.95° N, 124.64° E; 19.75 km). It relocates northwest to the north-central Xinlin District by the 2050s under SSP5-8.5 (51.94° N, 124.64° E; 110.60 km) and then to the western part by the 2070s (52.01° N, 124.34° E; 22.1 km).

This result reveals that *Quercus mongolica* predominantly migrates toward the northwest and to higher altitudes in different periods and climate scenarios, with the exception of a northeast shift in the 2070s under SSP1-2.6. The migration distance increases with higher greenhouse gas emissions over the same period, and the distance migrated in the 2070s is consistently shorter than that in the 2050s in each climate scenario.

4. Discussion

The niche model is based on the statistical correlation between species distribution and environmental variables and primarily focuses on significant environmental influences on species distribution but tends to overlook interspecies interactions, evolutionary processes, extreme disturbances, and species dissemination [72,73]. While the existing relationships between species and their environmental factors, particularly climatic conditions, may not consistently provide precise forecasts for the distribution of species in the future, niche modeling remains the predominant approach for analyzing the effects of climate change on species distributions within a region [19]. It is crucial to understand that these models predict potential suitable habitats for species, not their actual distribution. The interaction between species and their migration capabilities restricts the presence of specific species in certain areas, meaning that the actual distribution is only a part of the potential distribution [74]. Future research should more comprehensively consider factors such as vegetation competition and succession, botanical functional processes, and insect infestation impacts in order to develop and improve the integration techniques between regional climate models and dynamic ecosystem models.

4.1. Potential Current and Future Habitat Distributions

The Greater Khingan Range area is characterized by a typical cold temperate continental monsoon climate [75,76]. During winter, it is dominated by the Mongolian High, leading to temperature inversion and stable snow cover, which contribute to the region's significant permafrost heterogeneity [77]. The extreme low temperatures (reaching -52.3°C), prolonged winter snow cover (approximately five months), and the presence of permafrost pose substantial challenges to plant growth [78,79]. *Larix gmelinii*, as a principal constituent tree species of the cold temperate coniferous forests, exhibits high wood density and possesses notable frost resistance, enabling it to maintain elevated levels of water transport capacity in cold environments [80]. Furthermore, its well-developed root system can penetrate the permafrost to access water and nutrients, concurrently enhancing soil permeability and stability. These characteristics empower it to thrive in harsh environments. In contrast, *Quercus mongolica*, a secondary forest species, predominantly emerges in environments following the disturbance of primary forests. Its adaptability to environmental conditions may be comparatively lower [81].

Under the majority of future climatic scenarios, the suitable habitat of *Larix gmelinii* is anticipated to contract, with a trend of the distribution centroid shifting northwestward. This aligns with the conclusions derived by Zhang et al. [82] using the Maxent model, which predict a significant reduction in the suitable habitat of *Larix gmelinii* forests in northeast China during the 2050s and 2070s. Shi et al. [83] further corroborate this perspective, noting that under the effects of climate change, the suitability of *Larix gmelinii* in northeast China will decline, particularly in the eastern foothills of the Greater Khingan Range, the Lesser Khingan Range, and the Changbai Mountains. In these areas, the decrease in suitable habitat area is especially pronounced, with potential distribution areas expected to move northward and contract towards central regions. While many studies [82–85] have shown variability in the specific figures regarding the rate of habitat loss for *Larix gmelinii*, they collectively highlight a significant trend: under the overarching context of global warming and increased precipitation, the distribution area of *Larix gmelinii* is expected to contract, indicating its sensitivity and vulnerability to future climate change. The variations in these figures likely arise from differences in study areas, environmental factors, models, and parameter settings, which in turn limit the comparability of the results [86].

Conversely, *Quercus mongolica* shows considerable adaptability to future climatic changes, with all predictive scenarios indicating an expansion in its suitable habitat area. These findings are consistent with previous studies on climate change impacts in northeastern forests. For instance, Chen et al. [87] employed the ECHAM5-OM and HadCM3 atmospheric circulation models for simulations and revealed that climate warming over the next century (2002–2102) will favor birches and *Quercus mongolica* in northeastern forest communities. Similarly, Yan et al. [88] conducted simulations using the NEWCOP model under GFDL climate change scenarios for forests in the Greater Khingan Range and observed a gradual increase in the proportion of *Quercus mongolica*. Other studies, such as those referenced [89–91], consistently report that regional warming benefits the growth of temperate broadleaf forests. The expansion of *Quercus mongolica* forests is primarily attributed to its significant physiological traits. Firstly, the stability of this species is underpinned by its remarkable adaptability, resistance, and resilience, leading to a longer lifespan for *Quercus mongolica* and its ability to dominate habitats once it establishes a community [40,92,93]. Secondly, *Quercus mongolica* is among the most drought-tolerant species owing to its well-developed root system. Additionally, *Quercus mongolica* possesses drought-resistant leaf structures with strong stomatal closure capabilities, low water potential, and flexible regulatory mechanisms [94,95]. Among broadleaf trees, it also exhibits high stem water flow—attributable to its unique leaf morphology—high branching angle of branches, and a higher leaf area index, enabling it to effectively absorb more water and nutrients [96]. These physiological structures enable *Quercus mongolica* to maintain a high rate of photosynthesis even under future warming conditions. Compared to other species, it shows greater survivability in poor soils [95,97]. Moreover, projections indicate that the future distribution centroid of *Quercus mongolica* is expected to shift predominantly towards the northwest, a continuation of the migration trend observed in past research, which is highlighted by a study showing that from 1896 to 1986, the northern boundary of the broadleaf forests in Heilongjiang Province extended approximately 290 km towards the northwest [98].

4.2. Environmental Variables Affecting the Distribution of *Larix gmelinii* and *Quercus mongolica*

Larix gmelinii, owing to its preference for sunlight, cold tolerance, and high adaptability to soil and moisture [99], is significantly more influenced by temperature (contributing 62.2%) than by precipitation (contributing 18.3%). This finding is corroborated by previous research; for instance, Shi [83] discovered through probability of presence analysis that spring maximum temperature (contributing over 50%) and annual mean temperature are key factors influencing its distribution rather than spring precipitation. Similarly, Yang et al. [84] identified that the primary climatic factors affecting its geographic distribution are the mean temperature of the coldest month (contributing over 50%), annual

temperature range, annual radiation, and accumulated temperature of ≥ 5 °C. Although different studies vary in their data sources and methodologies, and the main climatic factors differ, a consistent conclusion is the predominance of temperature over precipitation.

Annual temperature, elevation, and precipitation are crucial factors affecting *Quercus mongolica*'s distribution, with temperature being the most significant at 64.7%. This finding is consistent with studies identifying similar influencing factors. For example, Yin et al. [100] found that annual precipitation (330–910 mm) and annual temperature differences greater than 29 °C were dominant influencing factors, and Jia et al. [101] emphasized the impact of rainfall and altitude. Zhou et al. [102] focused on the influence of low temperatures in May on natural regeneration. Despite differences in factor contributions, all factors were related to temperature, precipitation, and altitude. Our study's logistical response curves show a distinct threshold for annual precipitation for *Quercus mongolica*'s suitable areas and its adaptability to lower temperatures, aligning with its drought resistance and cold tolerance. The elevation range of *Quercus mongolica* identified in this study aligns with the data presented in *Flora of China* (Volume 22, p. 236) [79], noting that *Quercus mongolica* commonly grows at elevations below 600 m in northeast China. Complementary literature [103] indicates that this species predominantly occupies an elevation range of 250 to 400 m in the Greater and Lesser Khingan Ranges and is typically found on low mountain summits, ridges, and variously inclined slopes, which supports these findings.

4.3. Implications for Conservation

Larix gmelinii and *Quercus mongolica*, key species in the Greater Khingan Range, face various challenges and opportunities due to climate change. Therefore, we provide the following conservation recommendations:

Larix gmelinii has high sensitivity and vulnerability to climate shifts; thus, it is crucial to enhance monitoring and research. This involves mitigating climate impacts, improving pest control, and carefully planning human activities to protect its population and ecological services. For example, the projected 54.06% habitat reduction by the 2070s under the SSP5-8.5 scenario suggests the need for stronger conservation efforts, such as expanding reserves, promoting tree planting, and controlling pests.

Although *Quercus mongolica* is adaptable, it will face challenges, particularly as future suitable areas are predicted to be of lower quality. Conservation planning should account for future climate impacts and include strategies to improve current and future suitable habitats. The projected 20.35% habitat increase by the 2070s under SSP5-8.5 is promising, but the potential impact on other species and its adaptability to less suitable areas must be considered. Thus, conservation efforts should aim for a balance: ensuring species diversity and the species' ability to thrive in varied conditions.

5. Conclusions

We used the Maxent model to predict the current and future habitat distribution of *Larix gmelinii* and *Quercus mongolica* in the Greater Khingan Range under varying climate scenarios. Significant differences were observed in the species' responses to climate change. *Larix gmelinii* is projected to experience a reduction in its suitable habitat and a likely shift towards the northwest in future scenarios. In contrast, *Quercus mongolica* is expected to expand its habitat in all scenarios, mostly shifting northwest, demonstrating stronger adaptability.

Our findings provide a baseline for further research into the region's forest ecosystems and biodiversity conservation. The combination of GIS methods and Maxent modeling proved effective for developing conservation strategies. Future research should broaden niche modeling to include more tree species and use diverse climate models and environmental factors to enhance the distribution models to deepen our understanding of the Greater Khingan Range's forest response to climate change.

Author Contributions: Conceptualization, B.D. and D.Z.; methodology, B.D.; software, B.D.; validation, D.Z.; formal analysis, B.D.; investigation, X.L.; resources, B.D., X.L., X.W., X.Z. and X.W.; data curation, B.D. and X.L.; writing—original draft preparation, B.D.; writing—review and editing, B.D., D.Z. and Z.W.; project administration, B.D. All authors have read and agreed to the published version of the manuscript.

Funding: This research was funded by the National Natural Science Foundation of China (No. 41671064) and the Natural Science Foundation of Heilongjiang Province (No. LH2021D012).

Data Availability Statement: The data that support the findings of this study are not openly available but are available from the corresponding author upon reasonable request.

Acknowledgments: We acknowledge with great appreciation the technical support provided by Xi’an Keshuo Co., Ltd., Xi’an, China.

Conflicts of Interest: The authors declare no conflicts of interest.

Appendix A

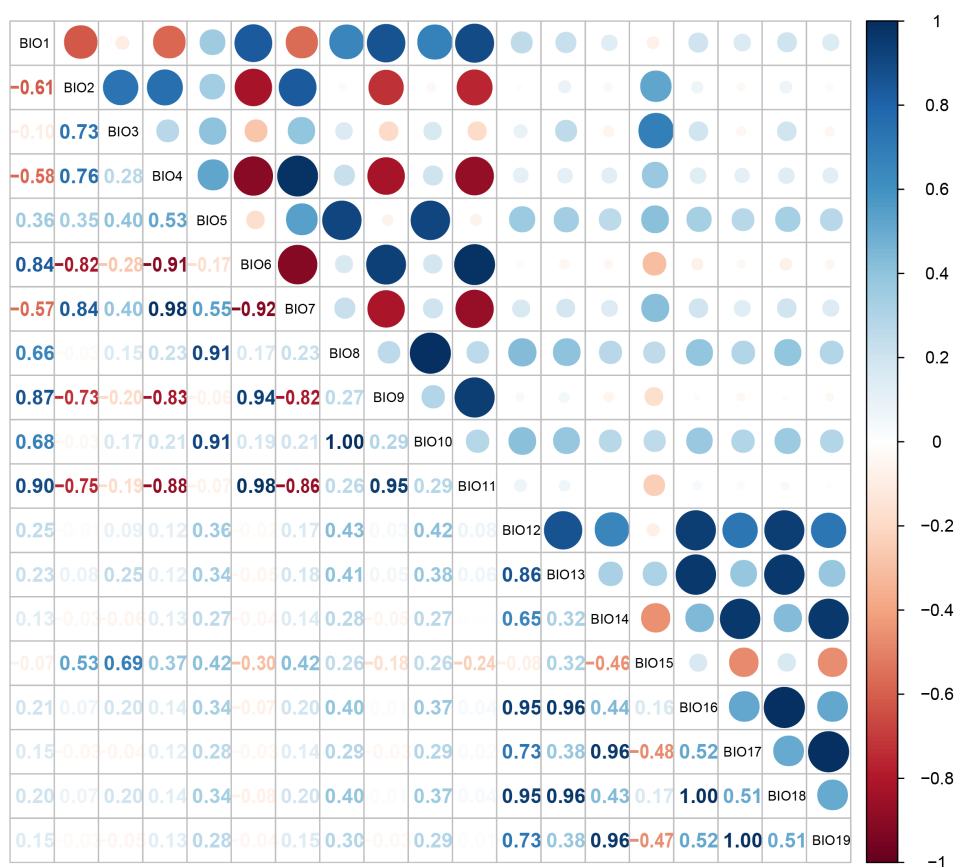


Figure A1. Assessing interrelations of 19 bioclimatic variables: Pearson’s (r) correlation analysis via ENM tools: $|r| \geq 0.8$ is displayed in bold.

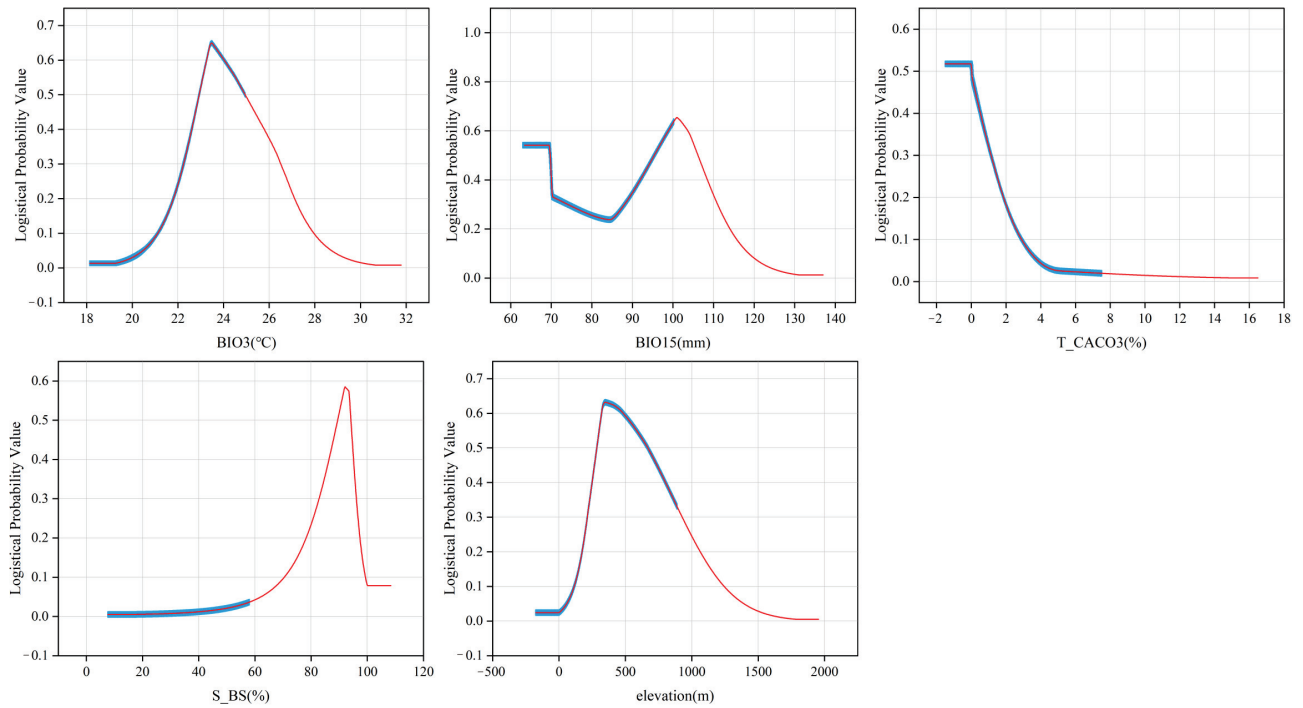


Figure A2. Response curves characterizing how variables affected the Maxent predictions for *Larix gmelinii*. Red lines represent logistical predictions varying with each climatic variable while holding other variables at their means. Shaded regions denote one standard deviation from this mean.

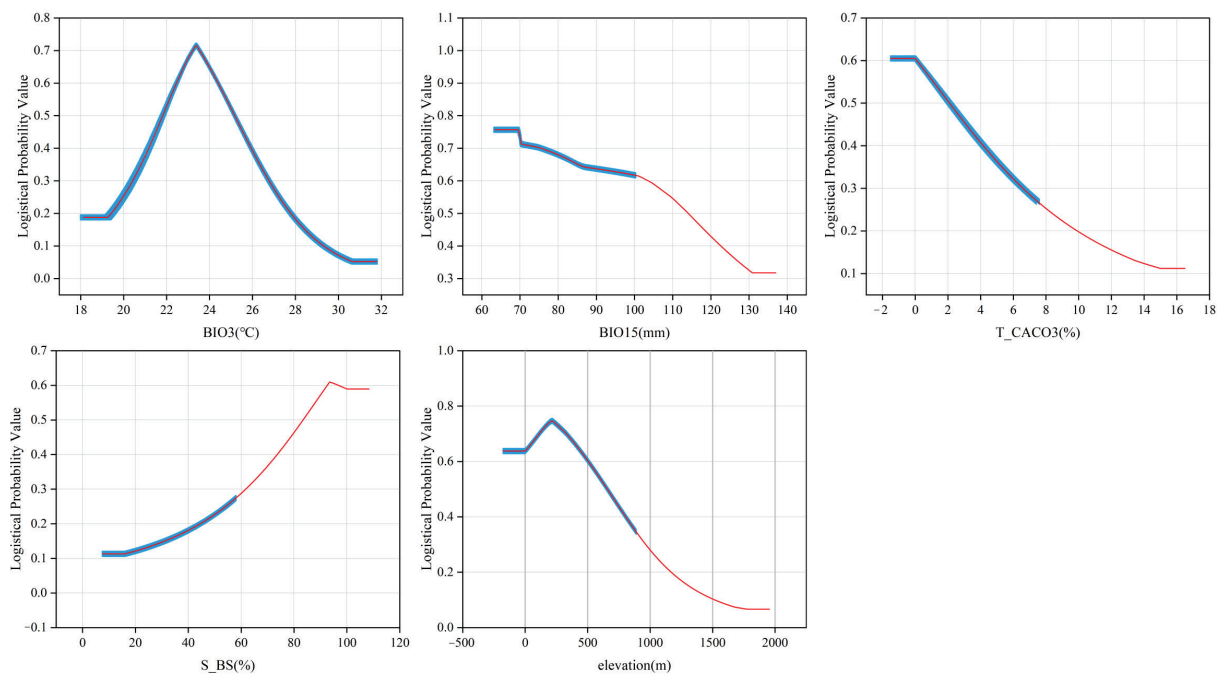


Figure A3. Response curves characterizing how variables affected the Maxent predictions for *Larix gmelinii*. Based on individual variables, the Maxent models generate red lines. Shaded regions denote one standard deviation from this mean.

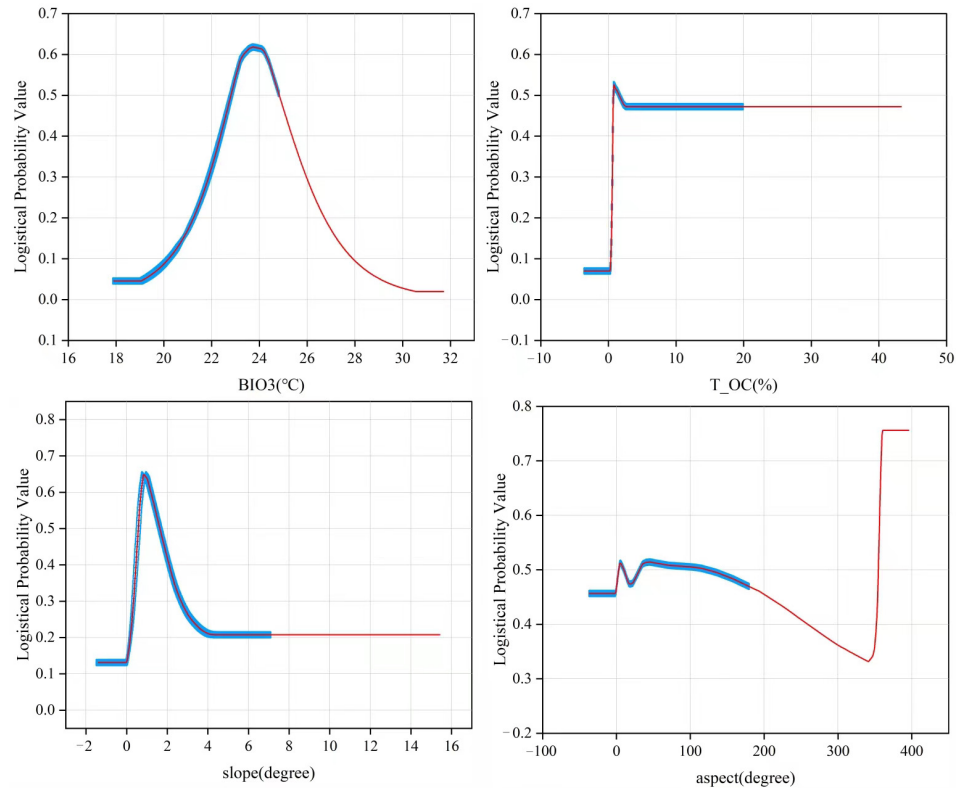


Figure A4. Response curves characterizing how variables affected the Maxent predictions for *Quercus mongolica*. Red lines represent logistical predictions varying with each climatic variable while holding other variables at their means. Shaded regions denote one standard deviation from this mean.

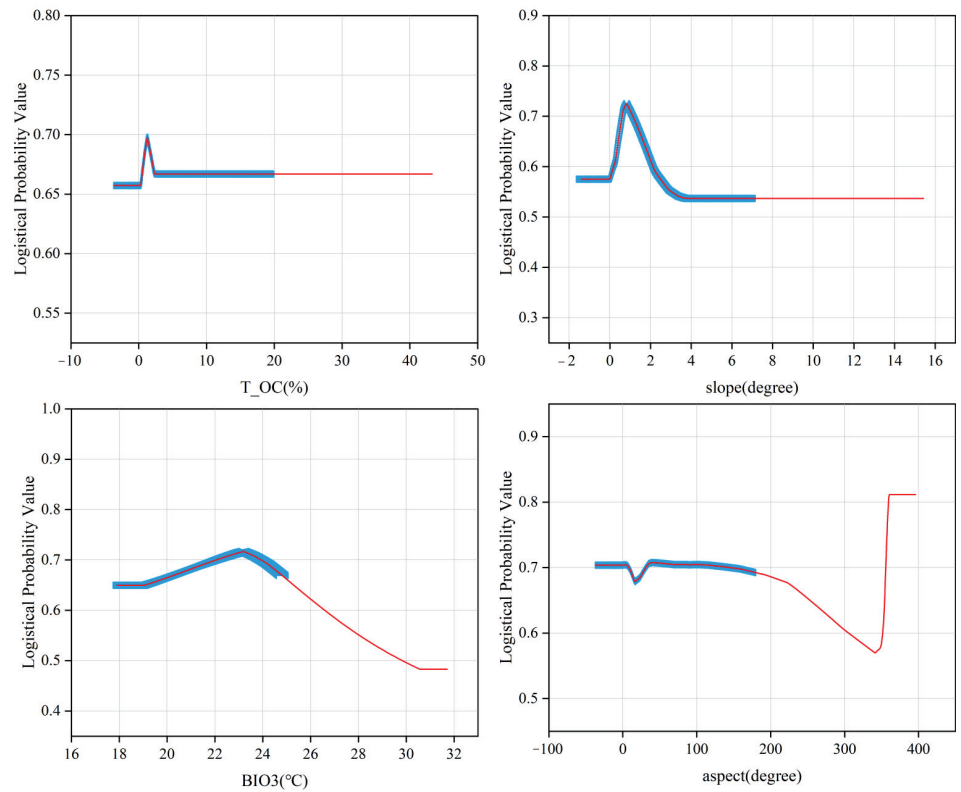


Figure A5. Response curves characterizing how variables affected the Maxent predictions for *Quercus mongolica*. Based on individual variables, the Maxent models generate red lines. Shaded regions denote one standard deviation from this mean.

Table A1. WorldClim version 2.1: standard 19 bioclimatic variables. The monthly values are averages over 20-year periods: 2021–2040, 2041–2060 and 2061–2080.

Variables	Description	Units
BIO1	Annual Mean Temperature	°C
BIO2	Mean Diurnal Range (mean of monthly (max temp – min temp))	°C
BIO3	Isothermality (BIO2/BIO7) × 100	/
BIO4	Temperature Seasonality (standard deviation × 100)	/
BIO5	Max Temperature of Warmest Month	°C
BIO6	Min Temperature for Coldest month	°C
BIO7	Temperature Annual Range (BIO5–BIO6)	°C
BIO8	Mean Temperature of Wettest Quarter	°C
BIO9	Mean Temperature of Driest Quarter	°C
BIO10	Mean Temperature of Warmest Quarter	°C
BIO11	Mean Temperature of Coldest Quarter	°C
BIO12	Annual Precipitation	mm
BIO13	Precipitation of Wettest Month	mm
BIO14	Precipitation of Driest Month	mm
BIO15	Precipitation Seasonality (Coefficient of Variation)	/
BIO16	Precipitation of Wettest Quarter	mm
BIO17	Precipitation of Driest Quarter	mm
BIO18	Precipitation of Warmest Quarter	mm
BIO19	Precipitation of Coldest Quarter	mm

References

- Hui, D.; Deng, Q.; Tian, H.; Luo, Y. Climate Change and Carbon Sequestration in Forest Ecosystems. *Handb. Clim. Chang. Mitig. Adapt.* **2017**, *555*, 555–594. [[CrossRef](#)]
- Ninan, K.N.; Inoue, M. Valuing forest ecosystem services: What we know and what we don't. *Ecol. Econ.* **2013**, *93*, 137–149. [[CrossRef](#)]
- Yu, P.; Richard, A.B.; Oliver, L.P.; Robert, B.J. The Structure, Distribution, and biomass of the World's Forests. *Annu. Rev. Ecol. Evol. Syst.* **2013**, *44*, 593–622. [[CrossRef](#)]
- IPCC. Summary for Policymakers. In *Climate Change 2021—The Physical Science Basis: Working Group I Contribution to the Sixth Assessment Report of the Intergovernmental Panel on Climate Change*; Intergovernmental Panel on Climate Change (IPCC), Ed.; Cambridge University Press: Cambridge, UK, 2023; pp. 3–32.
- Právělie, R. Major perturbations in the Earth's forest ecosystems. Possible implications for global warming. *Earth-Sci. Rev.* **2018**, *185*, 544–571. [[CrossRef](#)]
- Martinez del Castillo, E.; Zang, C.S.; Buras, A.; Hackett-Pain, A.; Esper, J.; Serrano-Notivol, R.; Hartl, C.; Weigel, R.; Klesse, S.; Resco de Dios, V.; et al. Climate-change-driven growth decline of European beech forests. *Commun. Biol.* **2022**, *5*, 163. [[CrossRef](#)]
- Mishra, S.N.; Gupta, H.S.; Kulkarni, N. Impact of climate change on the distribution of Sal species. *Ecol. Inform.* **2021**, *61*, 101244. [[CrossRef](#)]
- Paritsis, J.; Veblen, T.T. Dendroecological analysis of defoliator outbreaks on *Nothofagus pumilio* and their relation to climate variability in the Patagonian Andes. *Glob. Chang. Biol.* **2011**, *17*, 239–253. [[CrossRef](#)]
- Girardin, M.P.; Hogg, E.H.; Bernier, P.Y.; Kurz, W.A.; Guo, X.J.; Cyr, G. Negative impacts of high temperatures on growth of black spruce forests intensify with the anticipated climate warming. *Glob. Chang. Biol.* **2016**, *22*, 627–643. [[CrossRef](#)] [[PubMed](#)]
- Wang, J.; Taylor, A.R.; D'Orangeville, L. Warming-induced tree growth may help offset increasing disturbance across the Canadian boreal forest. *Proc. Natl. Acad. Sci. USA* **2023**, *120*, e2212780120. [[CrossRef](#)]
- Montoya-Jimenez, J.C.; Valdez-Lazalde, J.R.; Angeles-Perez, G.; de los Santos-posadas, H.M.; Cruz-Cardenas, G. Predictive capacity of nine algorithms and an ensemble model to determine the geographic distribution of tree species. *iForest-Biogeoosci. For.* **2022**, *15*, 363–371. [[CrossRef](#)]
- Hebbar, K.B.; Abhin, P.S.; Sanjo Jose, V.; Neethu, P.; Santhosh, A.; Shil, S.; Prasad, P.V.V. Predicting the Potential Suitable Climate for Coconut (*Cocos nucifera* L.) Cultivation in India under Climate Change Scenarios Using the Maxent Model. *Plants* **2022**, *11*, 731. [[CrossRef](#)] [[PubMed](#)]
- Yousaf, A.; Hadi, R.; Khan, N.; Ibrahim, F.; Moin, H.; Rahim, S.; Hussain, M. Identification of suitable habitat for *Taxus wallichiana* and *Abies pindrow* in moist temperate forest using Maxent modelling technique. *Saudi J. Biol. Sci.* **2022**, *29*, 103459. [[CrossRef](#)] [[PubMed](#)]
- Phillips, S.J.; Dudík, M. Modeling of species distributions with Maxent: New extensions and a comprehensive evaluation. *Ecography* **2008**, *31*, 161–175. [[CrossRef](#)]
- Elith, J.; Kearney, M.; Phillips, S. The art of modelling range-shifting species. *Methods Ecol. Evol.* **2010**, *1*, 330–342. [[CrossRef](#)]

16. Chen, B.; Zou, H.; Meng, X.; Wang, L.; Hao, X.; Kang, X.; Wang, C.; Zhang, X. Distribution Patterns and Change Prediction of Suitable Habitats for Chaihu (*Radix Bupleuri*) and Narrow-Leaved Chaihu (*Radix Bupleuri Chinensis*) in China under Climate Change. *Acta Ecol. Sin.* **2022**, *20*, 1–13.
17. Warren, D.L.; Wright, A.N.; Seifert, S.N.; Shaffer, H.B. Incorporating model complexity and spatial sampling bias into ecological niche models of climate change risks faced by 90 California vertebrate species of concern. *Divers. Distrib.* **2014**, *20*, 334–343. [[CrossRef](#)]
18. Schymanski, S.J.; Dormann, C.F.; Cabral, J.; Chuine, I.; Graham, C.H.; Hartig, F.; Kearney, M.; Morin, X.; Römermann, C.; Schröder, B.; et al. Process, correlation and parameter fitting in species distribution models: A response to Kriticos et al. *J. Biogeogr.* **2013**, *40*, 612–613. [[CrossRef](#)]
19. Li, Y.; Li, M.; Li, C.; Liu, Z. Optimized Maxent Model Predictions of Climate Change Impacts on the Suitable Distribution of *Cunninghamia lanceolata* in China. *Forests* **2020**, *11*, 302. [[CrossRef](#)]
20. Dakhil, M.A.; Xiong, Q.; Farahat, E.A.; Zhang, L.; Pan, K.; Pey, B.; Olatunji, O.A.; Tariq, A.; Wu, X.; Zhang, A.; et al. Past and future climatic indicators for distribution patterns and conservation planning of temperate coniferous forests in southwestern China. *Ecol. Indic.* **2019**, *107*, 105559. [[CrossRef](#)]
21. Fick, S.E.; Hijmans, R.J. WorldClim 2: New 1-km Spatial Resolution Climate Surfaces for Global Land Areas. *Int. J. Climatol.* **2017**, *37*, 4302–4315. [[CrossRef](#)]
22. Harris, R.M.B.; Grose, M.R.; Lee, G.; Bindoff, N.L.; Porfirio, L.L.; Fox-Hughes, P. Climate Projections for Ecologists. *Wiley Interdiscip. Rev. Clim. Chang.* **2014**, *5*, 621–637. [[CrossRef](#)]
23. Moss, R.H.; Edmonds, J.A.; Hibbard, K.A.; Manning, M.R.; Rose, S.K.; van Vuuren, D.P.; Carter, T.R.; Emori, S.; Kainuma, M.; Kram, T.; et al. The Next Generation of Scenarios for Climate Change Research and Assessment. *Nature* **2010**, *463*, 747–756. [[CrossRef](#)] [[PubMed](#)]
24. Fan, X.W.; Miao, C.Y.; Duan, Q.Y.; Shen, C.W.; Wu, Y. The Performance of CMIP6 Versus CMIP5 in Simulating Temperature Extremes over the Global Land Surface. *J. Geophys. Res. Atmos.* **2020**, *125*, e2020JD033031. [[CrossRef](#)]
25. Du, Q.; Wei, C.; Liang, C.; Yu, J.; Wang, H.; Wang, W. Maxent Model Analysis of the Response of 12 Pioneer Tree Species to Climate Change in Northeast China. *Acta Ecol. Sin.* **2022**, *42*, 9712–9725. [[CrossRef](#)]
26. Han, J.; Zhao, H.; Zhu, L.; Zhang, Y.; Li, Z.; Wang, X. A Comparative Study on the Response of Radial Growth of *Quercus mongolica* and *Pinus koraiensis* to Climate Change in the Xiaoxing'an Mountains. *Chin. J. Appl. Ecol.* **2019**, *30*, 2218–2230. [[CrossRef](#)]
27. Li, W.; Jiang, Y.; Dong, M.; Du, E.; Wu, F.; Zhao, S.; Xu, H. Species-specific growth-climate responses of Dahurian larch (*Larix gmelinii*) and Mongolian pine (*Pinus sylvestris* var. *mongolica*) in the Greater Khingan Range, northeast China. *Dendrochronologia* **2021**, *65*, 125803. [[CrossRef](#)]
28. Lyu, S.; Wang, X.; Zhang, Y.; Li, Z. Different responses of Korean pine (*Pinus koraiensis*) and Mongolia oak (*Quercus mongolica*) growth to recent climate warming in northeast China. *Dendrochronologia* **2017**, *45*, 113–122. [[CrossRef](#)]
29. Wang, C.; Gower, S.T.; Wang, Y.; Zhao, H.; Yan, P.; Bond-Lamberty, B.P. The Influence of Fire on Carbon Distribution and Net Primary Production of Boreal *Larix gmelinii* Forests in North-Eastern China. *Glob. Chang. Biol.* **2001**, *7*, 719–730. [[CrossRef](#)]
30. Huang, C.; Liang, Y.; He, H.S.; Wu, M.M.; Liu, B.; Ma, T. Sensitivity of Aboveground Biomass and Species Composition to Climate Change in Boreal Forests of Northeastern China. *Ecol. Model.* **2021**, *445*, 109472. [[CrossRef](#)]
31. Zhang, K.; Li, T.; Qu, Y.; Gao, F.; Lin, J.; Jiang, L. Analysis of Precipitation and Temperature Trends in the Great Xing'an Mountains Region. *Forests* **2018**, *34*, 8–14. [[CrossRef](#)]
32. Zhou, L.; Li, W.; Wang, W.; Zhang, X.; Li, W.; Li, X.; Li, Y.; Wang, Z.; Zhang, G.; Zhang, J. *Vegetation of the Daxinganling Region in China*; Science Press: Beijing, China, 1991.
33. Dong, L.; Liu, Z.; Li, F.; Jiang, L. Spatial Structure and Optimal Tree Species Composition of Major Forest Types in the Daxinganling Mountains. *For. Sci. Res.* **2014**, *27*, 6. [[CrossRef](#)]
34. Bai, X. Analysis of Point Pattern Distribution of Several Major Plant Species in Typical Forest Areas of the Daxinganling Mountains. *China High Technol. Enterp.* **2012**, 106–107. [[CrossRef](#)]
35. Zhou, Y.; Dong, S.; Nie, S. *Heilongjiang Tree Record*; Heilongjiang Science Press: Harbin, China, 1986.
36. Xu, H. *Forests of the Greater Khingan Mountains, China*; Science Press: Beijing, China, 1998.
37. Zhou, Y.; Yu, Z.; Zhao, S. Carbon Storage and Carbon Balance in Major Forest Ecosystems in China. *Chin. J. Plant Ecol.* **2000**, *24*, 518–522.
38. Gao, J.; Ao, W.; Liu, D.; Xiang, L.; Li, J.; Cheng, X. Origin and Biological Characteristics of Xing'an Larch in the Greater Khingan Mountains. *Inner Mong. Sci. Technol. Econ.* **2003**, *10*, 99–100.
39. Xu, Z.-Q.; Li, W.-H.; Liu, W.-Z.; Wu, X.-B. Study on the Biomass and Productivity of Mongolian Oak Forests in Northeast Region of China. *Chin. J. Eco-Agric.* **2006**, *14*, 21–24.
40. Wei, X.H. Comprehensive Study on Mongolian Oak Ecosystem. Ph.D. Thesis, Northeast Forestry University, Harbin, China, 1989.
41. Xu, Z.B. Study on the Root Distribution Patterns of Main Tree Species in the Broadleaf Korean Pine Forests of Changbai Mountain. *J. Ecol.* **1992**, *41*, 1924.
42. Wen, S.Y.; Yang, S.H.; Yin, Z.F.; Gao, H.Y.; Li, N.N.; Li, J.H.; Xia, J.; Luo, H.H.; Zhang, Q.X.; Bai, J.Y. Study on Canopy Structure, Light Distribution, and Leaf Growth in Oak Silkworm Forests. *J. Appl. Ecol.* **1991**, *2*, 286–291.
43. Wen, Z.D.; Yang, S.H.; Jiang, B.; Gao, H.Y.; Li, N.N.; Li, J.H.; Xia, J.; Luo, H.H.; Zhang, Q.X.; Bai, J.Y. Study on Biological Productivity and Substance Transformation of Oak Silkworm Forests. *J. Ecol.* **1993**, *12*, 5–10.

44. Chen, D.K.; Zhou, X.F. Structure, Function, and Succession of Four Types of Natural Secondary Forests. *J. Northeast For. Univ.* **1982**, *10*, 1–20.
45. Veloz, S.D. Spatially autocorrelated sampling falsely inflates measures of accuracy for presence-only niche models. *J. Biogeogr.* **2009**, *36*, 2290–2299. [[CrossRef](#)]
46. Brown, J.L. SDMtoolbox: A python-based GIS toolkit for landscape genetic, Biogeographic and species distribution model analyses. *Methods Ecol. Evol.* **2014**, *5*, 694–700. [[CrossRef](#)]
47. Tebaldi, C.; Debeire, K.; Eyring, V.; Fischer, E.; Fyfe, J.; Friedlingstein, P.; Knutti, R.; Lowe, J.; O'Neill, B.; Sanderson, B.; et al. Climate model projections from the Scenario Model Intercomparison Project (ScenarioMIP) of CMIP6. *Earth Syst. Dyn.* **2020**, *12*, 253–293. [[CrossRef](#)]
48. Fan, X.; Miao, C.; Duan, Q.; Shen, C.; Wu, Y. Future Climate Change Hotspots Under Different 21st Century Warming Scenarios. *Earths Future* **2021**, *9*, e2021EF002027. [[CrossRef](#)]
49. Xiao-Ge, X.; Tong-Wen, W.; Jiang-Long, L.; Zai-Zhi, W.; Wei-Ping, L.; Fang-Hua, W. How Well does BCC_CSM1.1 Reproduce the 20th Century Climate Change over China? *Atmos. Ocean. Sci. Lett.* **2013**, *6*, 21–26. [[CrossRef](#)]
50. Wu, T.; Li, W.; Ji, J.; Xin, X.; Li, L.; Wang, Z.; Zhang, Y.; Li, J.; Zhang, F.; Wei, M.; et al. Global carbon budgets simulated by the Beijing Climate Center Climate System Model for the last century. *J. Geophys. Res. Atmos.* **2013**, *118*, 4326–4347. [[CrossRef](#)]
51. Warren, D.L.; Seifert, S.N. Ecological Niche Modeling in MaxEnt: The Importance of Model Complexity and the Performance of Model Selection Criteria. *Ecol. Appl.* **2011**, *21*, 335–342. [[CrossRef](#)] [[PubMed](#)]
52. Jiménez-Valverde, A.; Lobo, J.M.; Hortal, J. Not as Good as They Seem: The Importance of Concepts in Species Distribution Modeling. *Divers. Distrib.* **2008**, *14*, 885–890. [[CrossRef](#)]
53. Radosavljevic, A.; Anderson, R.P. Making better MAXENT models of species distributions: Complexity, overfitting and evaluation. *J. Biogeogr.* **2014**, *41*, 629–643. [[CrossRef](#)]
54. Cobos, M.E.; Peterson, A.T.; Barve, N.; Osorio-Olvera, L. Kuenm: An R package for detailed development of ecological niche models using Maxent. *PeerJ* **2019**, *7*, e6281. [[CrossRef](#)]
55. Wintle, B.A.; McCarthy, M.A.; Parris, K.M.; Bugman, M.A. Precision and Bias of Methods for Estimating Point Survey Detection Probabilities. *Ecol. Appl.* **2004**, *14*, 703–712. [[CrossRef](#)]
56. Elith, J.; Phillips, S.J.; Hastie, T.; Dudík, M.; Chee, Y.E.; Yates, C.J. A Statistical Explanation of MaxEnt for Ecologists. *Divers. Distrib.* **2011**, *17*, 43–57. [[CrossRef](#)]
57. Zhao, H.; Xian, X.; Zhao, Z.; Zhang, G.; Liu, W.; Wan, F. Climate Change Increases the Expansion Risk of *Helicoverpa zea* in China According to Potential Geographical Distribution Estimation. *Insects* **2022**, *13*, 79. [[CrossRef](#)] [[PubMed](#)]
58. Hanley, J.A.; McNeil, B.J. The Meaning and Use of the Area Under a Receiver Operating Characteristic (ROC) Curve. *Radiology* **1982**, *143*, 29–36. [[CrossRef](#)]
59. Fielding, A.H.; Bell, J.F. A review of methods for the assessment of prediction errors in conservation presence/absence models. *Environ. Conserv.* **1997**, *24*, 38–49. [[CrossRef](#)]
60. Swets, J.A. Measuring the Accuracy of Diagnostic Systems. *Science* **1988**, *240*, 1285–1293. [[CrossRef](#)] [[PubMed](#)]
61. Li, L.H.; Liu, H.Y.; Lin, Z.S.; Jia, J.H.; Liu, X. Identifying Priority Areas for Monitoring the Invasion of *Solidago canadensis* Based on MAXENT and ZONATION. *Sci. Technol. Rev.* **2017**, *37*, 3124–3132. [[CrossRef](#)]
62. Warren, D.L.; Matzke, N.J.; Cardillo, M.; Baumgartner, J.B.; Beaumont, L.J.; Turelli, M.; Glor, R.E.; Huron, N.A.; Simões, M.; Iglesias, R.E.; et al. ENMTools 1.0: An R package for comparative ecological biogeography. *Ecography* **2021**, *44*, 504–511. [[CrossRef](#)]
63. Warren, D.L.; Glor, R.E.; Turelli, M. ENMTools: A toolbox for comparative studies of environmental niche models. *Ecography* **2010**. [[CrossRef](#)]
64. Steele, K.; Werndl, C. Climate Models, Calibration, and Confirmation. *Br. J. Philos. Sci.* **2013**, *64*, 609–635. [[CrossRef](#)]
65. Jiménez-Valverde, A.; Lobo, J.M. Threshold criteria for conversion of probability of species presence to either-or presence-absence. *Acta Oecol.* **2007**, *31*, 361–369. [[CrossRef](#)]
66. Xue, Y.; Lin, C.; Wang, Y.; Liu, W.; Wan, F.; Zhang, Y.; Ji, L. Predicting Climate Change Effects on the Potential Distribution of Two Invasive Cryptic Species of the *Bemisia tabaci* Species Complex in China. *Insects* **2022**, *13*, 1081. [[CrossRef](#)]
67. Liu, C.; Berry, P.M.; Dawson, T.P.; Pearson, R.G. Selecting Thresholds of Occurrence in the Prediction of Species Distributions. *Ecography* **2005**, *28*, 385–393. [[CrossRef](#)]
68. Jiao, X.; Long, M.; Li, J.; Yang, Q.; Liu, Z. Reconstructing the Invasive History and Potential Distribution Prediction of *Amaranthus palmeri* in China. *Agronomy* **2023**, *13*, 2498. [[CrossRef](#)]
69. Li, W.Q.; Xu, Z.F.; Shi, M.M.; Chen, J. Prediction of the Potential Geographic Distribution Pattern Changes of *Salix tetrasperma* under Different Climate Scenarios. *Acta Ecol. Sin.* **2019**, *39*, 3224–3234. [[CrossRef](#)]
70. Liao, J.F.; Yi, Z.L.; Li, S.C.; Xiao, L. Study on the Potential Distribution of *Dichanthium annulatum* Based on the Maxent Model in Different Periods. *Acta Ecol. Sin.* **2020**, *40*, 8297–8305. [[CrossRef](#)]
71. Zhang, Y.B.; Liu, Y.L.; Qin, H.; Meng, Q.X. Spatial Migration Prediction of Suitable Distribution Areas for *Elaeagnus mollis* under Climate Change Conditions. *Chin. J. Appl. Ecol.* **2019**, *30*, 496–502. [[CrossRef](#)]
72. Zhang, L. Estimation and Uncertainty Analysis of the Impact of Climate Change on the Geographic Distribution of Major Afforestation Tree Species/Natural Vegetation in China. Ph.D. Thesis, Chinese Academy of Forestry, Beijing, China, 2011.

73. Zhao, H.; Xian, X.; Liang, T.; Wan, F.; Shi, J.; Liu, W. Constructing an Ensemble Model and Niche Comparison for the Management Planning of Eucalyptus Longhorned Borer *Phoracantha semipunctata* under Climate Change. *Insects* **2023**, *14*, 84. [CrossRef]
74. Wang, W.; Gao, S.; Wang, S. Prediction of Potential Invasion Areas of Four Toxic Weeds in Grassland in Gansu. *Acta Ecol. Sin.* **2019**, *39*, 5301–5307.
75. Duan, B.; Man, X.; Cai, T.; Xiao, R.; Ge, Z. Increasing Soil Organic Carbon and Nitrogen Stocks along with Secondary Forest Succession in Permafrost Region of the Daxing'an Mountains, Northeast China. *Glob. Ecol. Conserv.* **2020**, *24*, e01258. [CrossRef]
76. Duan, L.; Cai, T. Changes in Magnitude and Timing of High Flows in Large Rain-Dominated Watersheds in the Cold Region of North-Eastern China. *Water* **2018**, *10*, 1658. [CrossRef]
77. Chang, X.; Jin, H.; He, R.; Zhang, Y.; Li, X.; Jin, X.; Li, G. Permafrost changes in the northwestern Da Xing'anling Mountains, Northeast China, in the past decade. *Earth Syst. Sci. Data* **2022**, *14*, 3947–3959. [CrossRef]
78. Cui, Y. Response of *Larix decidua* Radial Growth to Climate Change in the Da Xing'anling Region. Master's Thesis, Harbin Normal University, Harbin, China, 2020.
79. Editorial Committee of Flora of China, Chinese Academy of Sciences. *Flora of China*; Science Press: Beijing, China, 1998; Volume 7, pp. 187–237.
80. Zhang, X.; Bai, X.; Hou, M.; Chen, Z.; Manzanedo, R.D. Warmer Winter Ground Temperatures Trigger Rapid Growth of Dahurian Larch in the Permafrost Forests of Northeast China. *JGR Biogeosci.* **2019**, *124*, 1088–1097. [CrossRef]
81. Li, X.; Liu, W.S. Analysis of Secondary Forest Community Structure and Dominant Species Population Patterns in Mongolian Oak Forests. *Plant Res.* **2020**, *40*, 830. [CrossRef]
82. Zhang, X.; Chen, C.; Gao, F.; Yuan, S.; Han, S.; Ni, Z.; Yu, J. Spatial Distribution of *Larix gmelinii* Forests in Northeastern China and Their Response to Climate Change. *Ecol. J.* **2022**, *41*, 1041–1049. [CrossRef]
83. Shi, W. The Impact of Climate Change on the Distribution of *Larix gmelinii* in Northeastern China. Master's Thesis, Beijing Forestry University, Beijing, China, 2013.
84. Yang, Z.; Zhou, G.; Yin, X.; Jia, B. Geographic Distribution and Climatic Suitability of Natural *Larix gmelinii* Forests in China. *Ecol. J.* **2014**, *33*, 1429–1436. [CrossRef]
85. Li, F.; Zhou, G.S.; Cao, M.C. Simulation of the Geographic Distribution Response of Xing'an Larch to Climate Change. *J. Appl. Ecol.* **2006**, *17*, 2255–2260. Available online: <https://kns.cnki.net/KXReader/Detail?invoice=Qly4Q6b9ZAP3LZBcrJUA9zblekmd%2BSFeh9W5joB2lJd4SIJTWGqERCZFIG3HSLOYkNyzXj3JhUwsfM%2FyCtusi%2FHkK7ZnHdCPUkVYBLU%2Flc2GEN%2FRteE%2BmlZi0yytyueiFXJ%2BRtWtFw1%2FIK60T6j9FOW1GpT29DEU6PWOqgBF4lc%3D&DBCODE=CJFQ&FileName=YYSB200612004&TABLEName=cjfd2006&nonce=4943124702934F38AD474B51F15D23AE&TIMESTAMP=1705626680615&uid=> (accessed on 2 January 2024).
86. Zhang, L.; Liu, S.-R.; Sun, P.-S.; Wang, T.-L. Comparative evaluation of multiple models of the effects of climate change on the potential distribution of *Pinus massoniana*. *Chin. J. Plant Ecol.* **2011**, *35*, 1091–1105. [CrossRef]
87. Cheng, X.X.; Yan, X.D. Effects of Climate Change on Typical Forest in the Northeast of China. *Acta Ecol. Sin.* **2008**, *28*, 534–543.
88. Yan, X.D.; Zhao, S.H.D.; Yu, Z.H.L. Modeling Growth and Succession of Northeastern China Forests and Its Applications in Global Change Studies. *Acta Phytoecol. Sin.* **2000**, *24*, 1–8.
89. Zhao, S.D. Advance on the Study of Potential Impacts of Climate Change on Northeastern China Forest. *Acta Ecol. Sin.* **1995**, *15* (Supp. B), 1–9.
90. Liu, S.H.E. *Selected Works of Liu Shene*; Science Press: Beijing, China, 1985; pp. 7, 190, 195.
91. Chen, D.K.; Zhou, X.F.; Zhu, N. *Natural Secondary Forest—Structure, Function, Dynamics and Management*; Northeast Forestry University Press: Harbin, China, 1994; p. 237.
92. Yu, S.-L.; Ma, K.-P.; Chen, L.-Z. Preliminary Discussion on the Origin of *Quercus mongolica* Forest in North China. *Guihaia* **2000**, *20*, 131–137.
93. Xu, Z.Q.; Wang, Y.H. Progress in Research on *Quercus mongolica*. *Hebei J. For. Orchard Res.* **2002**, *17*, 365–370, ISSN 1007-4961.
94. Zheng, X.W.; Zhao, R.H.; Song, X.J. Research on Drought Resistance of Main Afforestation Tree Species in Western Liaoning Region. *For. Sci.* **1990**, *26*, 353–358.
95. Abrams, D.M.; Franzk, S. Does the Absence of Sediment Charcoal Provide Substantial Evidence against the Fire and Oak Hypothesis. *J. Ecol.* **1997**, *85*, 373–377. [CrossRef]
96. Wei, X.H.; Zhou, X.F. Study on Runoff of Three Types of Broadleaved Secondary Forests. *Acta Ecol. Sin.* **1989**, *9*, 325–332.
97. Abrams, D.M. Fire and the Development of Oak Forest. *Bioscience* **1992**, *42*, 346–353. [CrossRef]
98. Chen, X.-W. Characteristic Change of Several Forest Landscapes between 1896 and 1986 in Heilongjiang Province. *Acta Bot. Sin.* **2000**, *42*, 979–984.
99. Li, Z. *Natural Geography of the Northeast Region*; Higher Education Press: Beijing, China, 1993.
100. Yin, X.; Zhou, G.; Sui, X.; He, Q.; Li, R. Dominant Climatic Factors and Their Thresholds for the Geographic Distribution of Mongolian Oak. *Acta Ecol. Sin.* **2013**, *33*, 103–109.
101. Jia, X.; Ma, F.; Zhou, W.; Zhou, L.; Yu, D.; Qin, J.; Dai, L. The Impact of Climate Change on the Potential Geographic Distribution of Korean Pine Broad-Leaved Forests. *Acta Ecol. Sin.* **2017**, *37*, 464–473.

102. Zhou, X.; Zhang, Y.; Sun, H.; Chai, Y.; Wang, Y. The Impact of Climate Change on the Population Dynamics of Mongolian Oak in Northern Greater Khingan Mountains. *Acta Ecol. Sin.* **2002**, *7*, 1035–1040.
103. Li, X.; Liu, W.-S.; Zhou, W.; Chen, F.-Y.; Mu, L.-Q. Analysis on Community Structure and Dominant Population Point Pattern of Secondary Forest of *Quercus mongolica*. *Plant Res.* **2020**, *40*, 830–838. [[CrossRef](#)]

Disclaimer/Publisher’s Note: The statements, opinions and data contained in all publications are solely those of the individual author(s) and contributor(s) and not of MDPI and/or the editor(s). MDPI and/or the editor(s) disclaim responsibility for any injury to people or property resulting from any ideas, methods, instructions or products referred to in the content.